University of Central Oklahoma

Forensic Science Institute

The Wicking of Blood in Fabrics and the Effect It Has on the Angle of Impact

A Master's Thesis

Submitted to the Faculty

In partial fulfillment of the requirements for the

Degree of

Master of Science, Forensic Science

By

Lauren Duffle

Edmond, Oklahoma

Spring 2020

The undersigned have examined the thesis entitled **'The Wicking of Blood in Fabrics and the Effect It Has on the Angle of Impact'** presented by **Lauren Duffle**, a candidate for the degree of **Master of Science, Forensic Science** and hereby certify that it is worthy of acceptance.

4/1/2020	Mark R McCoy Digitally signed by Mark R McCoy Date: 2020.04.01 09:40:05 -05'00'	
Date	**Dr. Mark McCoy**	Committee Chairperson
4/1/2020	Wayne D. Lord Digitally signed by Wayne D. Lord Date: 2020.04.01 10:10:06 -05'00'	
Date	**Dr. Wayne Lord**	Committee Member
4/1/2020	Craig Gravel Digitally signed by Craig Gravel Date: 2020.04.01 13:49:11 -05'00'	
Date	**Mr. Craig Gravel**	Committee Member

Abstract

Bloodstain pattern analysis (BPA) is currently limited to smooth, non-porous surfaces. The purpose of this study was to determine whether the same mathematical model used to analyze bloodstain patterns on smooth, non-porous surfaces can be used to analyze bloodstains on non-smooth, porous surfaces (fabrics). This study used a control surface (poster board) and two fabric types, 100% cotton fabric and 98% cotton and 2% spandex fabric. Drops of non-coagulated pork blood were deposited onto all three surfaces at varying angles from 10 to 90 degrees at 10 degree increments, and the resulting bloodstains were measured using digital calipers and a drafting divider. A statistical analysis was done on the measurements using ANCOVA to test for differences between the mean absolute differences of the angles with respect to type of surface and actual angle, and Tukey's multiple comparisons was used when appropriate. The results showed that the same mathematical model used for smooth non-porous surfaces could be used to determine the angle of impact (AOI) for both fabrics tested, with a variance of no greater than +/- 5°. This could prove invaluable as a means of advancing the field of BPA.

Table of Contents

Table of Figures

Chapter One: *Introduction*

Bloodstain pattern analysis (BPA) is a form of crime scene reconstruction. A bloodstain analyst looks at a crime scene where blood evidence is present and, using that evidence and certain known factors effecting bloodstain patterns and transfers, determines the sequence of events that occurred. Multiple experiments done on blood have been shown to be reproducible. This is because, like all matter, blood obeys the laws of physics and, by applying the laws of physics and mathematical principles, researchers can calculate different effects on a droplet of blood in flight. According to Metcalf, a drop of blood in flight forms into a sphere due to surface tension (1980). The forces that act upon the droplet in flight will cause oscillations, but the viscosity of blood dampens these forces, allowing the droplet to maintain its spherical shape. The droplet also maintains the same volume throughout flight unless acted upon by some other force.

Understanding these factors leads to an understanding of what happens when a droplet impacts a surface. Bloodstain analysts can use these known factors about blood to compare to unknown bloodstains found at crime scenes. To obtain reproducible results, the surfaces studied in lab experiments were smooth and nonporous; therefore, unknown stains found at a scene are documented from smooth, non-porous surfaces for comparative results. However, the knowledge garnered by bloodstain patterns is severely limited, because there is not enough prior research to expand this branch of forensic science to include analysis of bloodstains on porous surfaces, such as fabrics, to recreate a crime scene.

There are a number of factors that can affect bloodstain patterns on porous surfaces. Depending on the composition and construction of a given fabric, blood droplets can absorb or

adsorb. Natural fibers with less dense construction will typically absorb bloodstains, retaining the original shape and general size of the bloodstain. Synthetic fibers and denser weaves will typically adsorb bloodstains, leading to a distortion of the size and shape of the bloodstains. Another significant factor affecting bloodstains on porous surfaces is curvature of fabrics. This is especially important when analyzing worn-clothing present at the time of a bloodshed event. The curvature of the fabrics can distort bloodstains and can often lead to incorrect assumptions about the type of blood evidence found. Other factors such as fabric age, condition and laundering can alter bloodstain patterns.

All of these issues complicate the analysis of bloodstains on fabrics, and there are no known, reproducible results to compare blood evidence to. It is imperative that forensic science continues to research and expand training on these issues in order to provide the most accurate depiction of a crime scene possible. To that end, this thesis project endeavored to determine if the same mathematical principles used to analyze bloodstain patterns on smooth, non-porous surfaces could be used to investigate bloodstain patterns on porous surfaces, namely denim and cotton.

Statement of the Problem

Currently, bloodstain analysts are unable to use bloodstain evidence found on non-smooth, porous surfaces to definitively determine angle of impact (AOI), an important aspect of crime scene reconstruction. The majority of prior research conducted on bloodstain patterns has solely focused on blood deposited on smooth, non-porous surfaces. This is because there are innumerable factors that can complicate BPA on non-smooth, porous surfaces, such as fabrics.

The most common factor that can complicate BPA on non-smooth, porous surfaces is fabric composition. There are two basic fiber types; natural and synthetic. However, there are countless combinations of fiber types used in the production of fabrics. Fabrics can be composed of both natural and synthetic fibers. Natural fibers will typically absorb bloodstains, whereas synthetic fibers will typically adsorb bloodstains. Absorption can cause distortion in the size of bloodstains, while adsorption can cause distortion in both the size and shape of bloodstains.

The next factor that can cause complications in BPA is fabric construction. There are two basic fabric constructions; weave and knit. As with fabric composition, there are myriad patterns of fabric weave and knit. Knit materials are constructed using interlocking loops. These interlocking loops allow fabric to stretch, which can lead to distortion in the size and shape of bloodstains between the point of deposition and the point of analysis. Woven fabrics are constructed by interlacing yarn at right angles to form the grain and have less stretch compared to knit fabrics. It is more difficult for small-volume bloodstains to penetrate either type of fabric construction if the fibers are densely packed.

The three-dimensionality of fabrics can also complicate BPA. This element affects the directionality of bloodstains. Bloodstains found on clothing worn during a blood shed event can be misinterpreted when analyzed on a flat surface. Wrinkles in fabrics can create three-dimensional surfaces upon which blood is impacting at different angles and at different times, resulting in non-elliptical stains.

Background and Need

Currently, blood evidence can provide law enforcement with a wealth of knowledge such as direction of travel, AOI, height the blood originated from, and much more. At a crime scene,

an analyst will document blood from smooth, non-porous surfaces because those samples can be compared to known reproducible results. Because few experiments have been done on blood when it impacts a porous surface, there are limited known results for which unknown samples can be compared. Successful research on the acceptability of AOI calculations taken from a porous surface stands to increase the number of usable bloodstain droplets that can be documented from a blood shed event.

Misty Holbrook performed a study evaluating blood deposition on fabrics, specifically trying to identify how to distinguish spatter and transfer stains (2010). She tested 11 fabrics, and each was hung in front of a larger piece of cardboard as a control. Using a rat trap, spatter patterns were created across the fabrics and control. Both the size and shape of the spatter stains on the fabrics were compared to the control. Next, Holbrook created transfer stains on the same 11 fabric types using various items in a lateral swiping motion to produce stains in the size range corresponding to the spatter. With one exception, Holbrook found the sizes were consistent with the control, and the shapes of the stains were diverse. Holbrook determined that with smaller volumes of blood, the differences between spatter and transfer stains became less apparent. This study focused on the appearance of bloodstains on multiple fabric types, but no quantitative results were garnered.

Dr. Mark Reynolds and Edmund Silenieks expanded on Holbrook's study and noted additional considerations when assessing bloodstains on fabrics (2016). They discussed the effects of both fabric composition and fabric construction on the appearance of bloodstains in reference to Holbrook's original study. Their research explains that woven materials are created with at least two yarns interlaced perpendicular relative to each other, and knitted materials are

created with at least one yarn forming interlocking loops. Knitted materials have more stretch than the woven materials and this stretch could distort the target surface.

Reynolds and Silenicks then added an additional consideration to the evaluation of bloodstains. They studied the effect of curvature of fabrics on bloodstains. They demonstrated these effects by dropping blood at 90-degree angles onto a curved surface. The directionality of the stains was vastly different. This study again focused on the appearance of bloodstain and did not attempt to determine the mathematical principles necessary to evaluate the AOI.

While all of these studies looked at variables studied in this thesis, none of them looked beyond the qualitative property of appearance which is of value when determining the pattern of bloodstain spatter on porous surfaces. However, they do little to advance the field of BPA in regards to the determination of quantitative properties such as AOI or area of origin.

Purpose of the Study

This study focused on the AOI of blood patterns on porous surfaces. The experiment endeavored to answer whether blood impacting a fabric surface provided acceptable results using the same mathematics as stains on smooth, nonporous surfaces. Because the surfaces were porous, wicking is known to affect the size and shape of the stain. While the measured AOI on smooth, two-dimensional surfaces is not perfectly precise due to measurement error, the measured AOI on *fabric* surfaces introduces additional sources of error (beyond the measurement errors on smooth, two-dimensional surfaces) based on the three-dimensional characteristics of the fabric surface. A control was used to validate the experimental design and setup while two commonly encountered fabrics were tested using accepted angle calculation methods for smooth, non-porous surfaces. All three substrates were then compared to the actual

experimental setup angle using the acceptability criteria of +/- 5° set forth by Gardner & Ross (1990) for acceptable calculated angle difference.

Research Questions

There were many questions that come to mind when proposing and designing this experiment. The most important question was, can the same mathematics used to determine the AOI on smooth, non-porous surfaces be used to determine the AOI on non-smooth, porous surfaces, such as fabrics? If the same mathematics cannot be used, can an analytical model be created that leads to reproducible results?

Significance to the Field

This experiment could prove to be invaluable and add to the growing knowledge base of bloodstain analysts. If the results prove to be acceptable, more bloodstain clothing evidence can be taken and analyzed from future crime scenes, providing additional clarity about the nature and sequence of events leading up to, and following, a bloodshed event.

Definitions

- Absorption – The interaction of blood on natural fibers. The blood penetrates the fiber and wicks as it saturates each fiber.
- Adsorption – The interaction of blood on synthetic fibers. The blood coats the outside of the fiber and wicks along the surface of each fiber.
- Angle of Impact – The acute angle (alpha), relative to the plane of a target, at which a blood drop strikes the target.

- Area of Convergence – The space in two dimensions to which the directionalities of spatter stains can be retraced to determine the location of the spatter producing event.
- Area of Origin – The space in three dimensions to which the trajectories of spatter can be utilized to determine the location of the spatter producing event.
- Blood Clot – A gelatinous mass formed by a complex mechanism involving red blood cells, fibrinogen, platelets, and other clotting factors.
- Bloodstain – A deposit of blood on a surface.
- Directionality – The characteristic of a bloodstain that indicates the direction blood was moving at the time of deposition.
- Drip Stain – A bloodstain resulting from a falling drop that formed due to gravity.
- Edge Characteristic – A physical feature of the periphery of a bloodstain.
- Impact Pattern – A bloodstain pattern resulting from an object striking liquid blood.
- Parent Stain – A bloodstain from which a satellite stain(s) originate.
- Satellite Stain – A smaller bloodstain that originated during the formation of the parent stain as a result of the blood impacting a surface.
- Saturation Stain – A bloodstain resulting from the accumulation of liquid blood in an absorbent material.
- Spatter Stain – A bloodstain resulting from an airborne blood drop created when external force is applied to liquid blood.
- Spines – An edge characteristic of bloodstains consisting of narrow elongated projections from the central area of the stain.

- Swipe – A bloodstain resulting from the transfer of blood from a blood-bearing surface onto another surface, with characteristics that indicate relative motion between the two surfaces.
- Target – A surface onto which blood has been deposited.
- Transfer Stain – A bloodstain resulting from contact between a blood-bearing surface and another surface.

(Organization of Scientific Area Committees for Forensic Science, 2017)

Limitations

This study cannot test all the possible combinations of fabric construction and composition. Fabric type and construct can affect how blood interacts with fabric. Each fiber type and construct needs to be examined individually against a control to build a pool of reproducible data.

This project was done in a laboratory setting where the environment was controlled. At a crime scene, blood evidence must be documented from an area or object that has some permanency or documented with photographs well enough to replicate the scene. A fitted sheet on a bed is less likely to be altered than a pillow that can be easily moved or curtains that can be moved by air flow. Good documentation is vital when looking for a pattern and area of convergence.

This project used pork blood from a local butchery to eliminate any effects anticoagulants might have on the wicking process. Once outside the body, blood is affected by environmental conditions and as time passes, the blood will clot and become unusable. The blood used in this

experiment was stirred continuously to inhibit the clotting factor and a new source of pork blood was collected for each sample set tested.

Droplets on smooth, non-porous surfaces sometimes contain features such as spines and tails. These features are not included in the length and width, and it is generally the decision of a bloodstain analyst what portion of a stain is to be measured. Droplets on porous surfaces, such as fabrics, have less distinguishing spine and tail features due to the wicking factor and require a higher skill level to determine what portion needs to be measured.

The biggest limitation in any BPA research is the researcher. The AOI in this study was found by measuring droplets with calipers. Depending on the skill level and work experience of future analysts, the results could differ from analyst to analyst. This potential problem is solved by understanding that the point of origin is actually an area and that the acceptable range of error is +/- 5°.

Chapter Two: *Review of the Literature*

Introduction

Currently, investigators are unable to use bloodstain evidence from non-smooth, porous surfaces when analyzing a crime scene due to lack of prior research in this area of forensic science. There are no reproducible results or analytical models that can provide definitive results for these kinds of bloodstains. There are innumerable variables that complicate analysis of bloodstains found on non-smooth, porous surfaces. These variables include fabric construction, fabric composition, and fabric curvature, all factors which can cause distortions in the size and shape of bloodstains.

This literature review covers three areas related to BPA on non-smooth, porous surfaces. The first section covers the basic principles surrounding BPA. The second section covers prior research conducted to ascertain the effect of fabric construction and composition on the appearance of bloodstain patterns left by blood spatter and blood transfer. The third section covers further research conducted investigating the effects of fabric construction, fabric composition, and fabric curvature on the misclassification of bloodstain evidence.

Bloodstain pattern analysis

It is important for crime scene analysts to have at least a basic understanding of BPA in order to properly assess scenes where bloodshed events have occurred. According to Gardner (2012), the discipline of BPA considers the location, shape, size, distribution, and other physical characteristics of bloodstains in the scene and, from this, derives information regarding the nature of the event that created the pattern. Blood as a fluid responds to variations of internal and external forces in a predictable fashion. The predictability of how blood behaves under basic

known conditions allows the unknown patterns to be compared via known classifications. This predictability also allows the analyst to recognize other aspects such as direction, impact angle and the alterations brought about by environmental conditions. There are three principles that bloodstain pattern analysts follow in BPA.

Pattern diversity principle.

The first of these principles, the pattern diversity principle, is articulated by Gardner as: "the variations in combinations of blood volumes and forces acting on those volumes lead to recognizable classes of patterns" (2012). The class pattern used in this experiment is static blood dispersed from a point source. This event mechanism can be described as a volume of blood present at a point source that is exposed to external forces to produce a pattern of small circular and elliptical-shaped stains referred to as impact patterns.

Principle of stain shape and directionality correlation.

Second is the principle of stain shape and directionality correlation. Gardner explains this principle as "…the shape of certain bloodstains provides indicators as to the direction of deposition as well as to the spatial origin of the blood" (2012). The analyst looks at two subprinciples, directionality and impact angle. The first consideration is directionality which is defined by the author as "the collapse of a free flight droplet on a surface [that] produces a stain with a circular or elliptical shape" (Gardner, 2012). Often, these shapes are accompanied by spines, scallops, or satellite marks, which can help determine the flight path of a droplet of blood. When multiple, related droplets are considered together, investigators can create a two-dimensional area called the

convergence point by back projecting through the long axis of each droplet from the same bloodshed event. Using the impact angle of each droplet from the same bloodshed event, the area of origin would be the area above the convergence point in the three-dimensional plane. The impact angle can be defined as the angle at which the droplets radiate from the area of origin and impact a surface. The math associated with AOI may seem complex but the application is simple when using a scientific calculator.

The next consideration Gardner discusses is the AOI which was first demonstrated by Balthazard in 1939 establishing a correlation between the AOI and the length of the long and short axes of a bloodstain. In 1982, MacDonell was able to create a mathematical model based upon the older, Balthazard principle. The model demonstrates that the trajectory of a blood droplet, when terminating on a flat surface, creates a right triangle. The length of the stain, also called the long axis, forms the hypotenuse of the right triangle, while the width of the stain, also called the short axis, creates the side opposite. The measurements of the long and short axes, or the length and width of the stain, are useful when determining the angle of the side adjacent, which is in actuality the AOI. In basic math terms, the width of the stain is divided by the length to determine *N* which is always a number less than 1. The inverse Sine of *N* is then calculated to determine the AOI.

This calculation, when taken along with the directionality of a bloodstain, can create a 3D model, which is vital in determining the origin of the blood splatter. This experiment will look at the directionality and how the wicking affects the shape of the stain. If the shape of the stain is distorted, then the AOI will also be askew.

Physically altered bloodstain principle.

The last principle is the physically altered bloodstain principle, and Gardner describes this principle as: "…once exposed, blood will react to environmental conditions in a predictable manner" (2012). This principle recognizes that blood dries, wicks, permeates, and coagulates in and on surfaces in a predictable manner. This experiment will look at how blood reacts when impacting different fabric surfaces.

Prior Research on the Appearance of Bloodstain Patterns

In her article focusing on the deposition of bloodstains on fabric, Misty Holbrook performed an experiment on 11 types of fabrics commonly used in manufacturing clothing in order to determine the changes of physical characteristics of bloodstains between different fabrics and fabric compositions left by blood spatter and blood transfer (2010). The methods Holbrook used involved 11 fabric types and a rat trap placed 2 feet at a right angle from a target. The blood was warmed to body temperature, and the clothing was suspended from a target and partially covered with cardboard to provide a control. The resultant stains were allowed to air dry and then analyzed using microscope.

The sizes of the stains on most fabrics were consistent with the stains from the covered, control portions of the cardboard. The only significant variance from the control stains occurred in the polyester material fabric. The shapes of the stains were more significantly impacted compared to the control stains on the cardboard. The rayon and nylon fabrics showed very few irregularities when compared to the control stains. Similarly, the cotton, cotton-blend, and silk fabric stains kept their shape, especially when the construction of the material weave was denser. Bloodstains on the wool and acrylic fabrics, however, were more likely to lose their original

shapes. Again, the most significant distortion in shape occurred in the polyester material, with the stains becoming larger and more elongated.

Holbrook also studied the effect of spatter versus transfer stains on each of the fabrics (2010). She determined the differences between the two types of stains were less apparent with smaller amounts of blood, because it was unable to penetrate certain fabrics or weaves. When there was a sufficient amount of blood applied to fabrics with a denser weave, such as silk or cotton-polyester blend, it was able to penetrate the fabric to create spatter-like patterns.

The results of the experiment showed that the size of the spatter, coupled with fabric type and construction, can lead to erroneous class patterns of transfer stains as spatter stains. She states that multiple stains should be examined, and all relevant factors should be taken into consideration in order to correctly identify the type of stain present.

Misclassification of Bloodstain Evidence

Dr. Mark Reynolds and Edmund Silenicks expanded upon Holbrook's experiment in a subsequent journal article (2016). The authors begin by discussing the importance of correctly identifying "activity evidence bloodstains" when investigating violent crimes.

It is often difficult to classify bloodstains on fabrics because the principles generally governing blood pattern analysis are only truly reliable when applied to smooth, static, non-porous surfaces. There are a number of factors the authors discuss that can complicate analysis, such as "fabric construction, composition, history, treatment(s), moisture content, [and] surface curvature or folding" (Reynolds & Silenieks, 2016).

As Holbrook demonstrated, composition and absorbency can affect the shape of blood spatter, while the shape of drip stains can be affected by factors like laundering, composition and structure. The authors introduced a new element not previously addressed in Holbrook's experiment, namely how curvature can affect directionality of bloodstain patterns. This factor is significant when analyzing worn clothing, often causing erroneous classifications and interpretations of bloodstains.

Reynolds & Silenieks then discuss preferential diffusion, focusing on the differences between natural and synthetic fibers (2016). Natural fibers typically absorb bloodstains, leading to a more accurate representation of deposition. Synthetics fibers, on the other hand, typically adsorb, meaning that blood droplets can only coat the surface of the fibers and wick along the synthetic yarns, causing an irregular bloodstain on the fabric.

The next topic the authors discuss is the effect fabric construction (i.e. weave vs. knit) has on the appearance of bloodstains. Woven fabrics are typically comprised of two strands of yarn, interwoven perpendicularly, while knit fabrics are typically comprised of one strand laced together in loops. Weaves tend to be sturdier while knits tend to have more stretch.

The composition of fabrics can lead to erroneous interpretations of bloodstain patterns if the stains are not examined microscopically. It is common for blood transfers on synthetic fibers to mimic impact spatter, which can further muddy a forensic investigation.

The authors conclude by stating the importance of training for technicians analyzing bloodstains on fabrics. It is a vital, developing field, and more research (and training) is needed to provide an accurate and thorough analysis of blood patterns in crime scenes.

Summary

It is readily apparent from the literature that there is a need for further research before bloodstain analysts can use bloodstain evidence collected from non-smooth, porous surfaces to obtain definitive results about a crime scene. The literature in this review examines many factors that can complicate BPA. Fabric construction, composition, and curvature can alter the appearance of bloodstains, leading to erroneous conclusions about the circumstances surrounding a blood shed event. However, the prior research only examined qualitative results. In order to advance the sub-field of BPA, research in which quantitative results are obtained must be conducted. To that end, this study focuses on the measurable effects of fabric construction and composition on bloodstains.

Chapter Three: *Methods*

Introduction

Very little prior research has been conducted that examines the quantitative effects of fabric construction and composition on bloodstain patterns. Due to this, bloodstain analysts are unable to draw definitive conclusions about the circumstances surrounding a blood shed event involving stains on fabric. In order to bridge this gap in forensic science, it must be determined whether the only existing mathematical model and evidence documentation methodology can be used to determine the AOI of blood spatter evidence deposited on both smooth, non-porous surfaces and non-smooth, porous surfaces, such as fabrics. If these cannot be used for blood spatter evidence deposited on non-smooth, porous surfaces, it must be determined whether a new model and evidence documentation methodology can be developed that will yield reproducible and accurate AOI results, within the accepted criteria of +/- 5°. This study focused on the quantitative results obtained from varying the AOI for blood spatter deposited on two common fabric types.

Warm, un-clotted blood was dropped from a micropipette onto the control surface and the two fabric types at multiple, controlled angles. The bloodstains were then measured, and the measurements were analyzed to determine the variance between the calculated AOI (from the fabric samples) and the actual AOI (built into the experimental setup). A smooth, non-porous control surface was also measured and compared to the actual AOI to validate the experimental design yielded results within the accepted criteria of +/-5°.

Setting

The experiment was conducted at the University of Central Oklahoma, in the bay of the Forensic Science Institute. The bay is a climate-controlled, laboratory space designated for research experimentation in multiple forensic science disciplines.

Intervention and Materials

Usually, bagged blood, which contains an anticoagulant, is used for experiments, but for realistic purposes, the blood used in this experiment was obtained from a local butcher shop and continuously stirred to prevent clotting due to the absence of anticoagulant.

Poster board was used as the control because it has a smooth, nonporous surface, and the results are known to be reproducible. Two common fabrics were selected; a 100% cotton fabric, and a denim fabric, composed of 98% cotton and 2% Spandex. The fabrics were washed six times with Tide and ironed before performing the experiment. See **Figure 1** - **Figure 3**.

Figure 1: Control - Poster board, Glossy

Figure 2: Fabric 1 - Bed sheet, 100% Cotton

Figure 3: Fabric 2 - Jeans, 98% Cotton, 2% Spandex

A miter saw was used to cut angles into a two-by-four at 10-degree increments ranging from 10 degrees to 80 degrees with the 90 degree position being laid directly on the floor. A close-up of the two-by-four can be seen in **Figure 4**. A clipboard was inserted into a cut angle of the two by four and used to hold the control and sample fabrics while blood was being deposited.

Figure 5 shows clipboards inserted all at once to show each angle; however, only one clipboard was used at a time during the experiment. A 0.5ml micropipette, see **Figure 6**, was used to drop the blood because it allowed the blood to drop due to gravity instead of using force from the plunger to expel the droplet.

Figure 4: Experimental setup showing angled slots of 80 to 10 degrees

Figure 5: Experimental setup with clipboards inserted into each slot

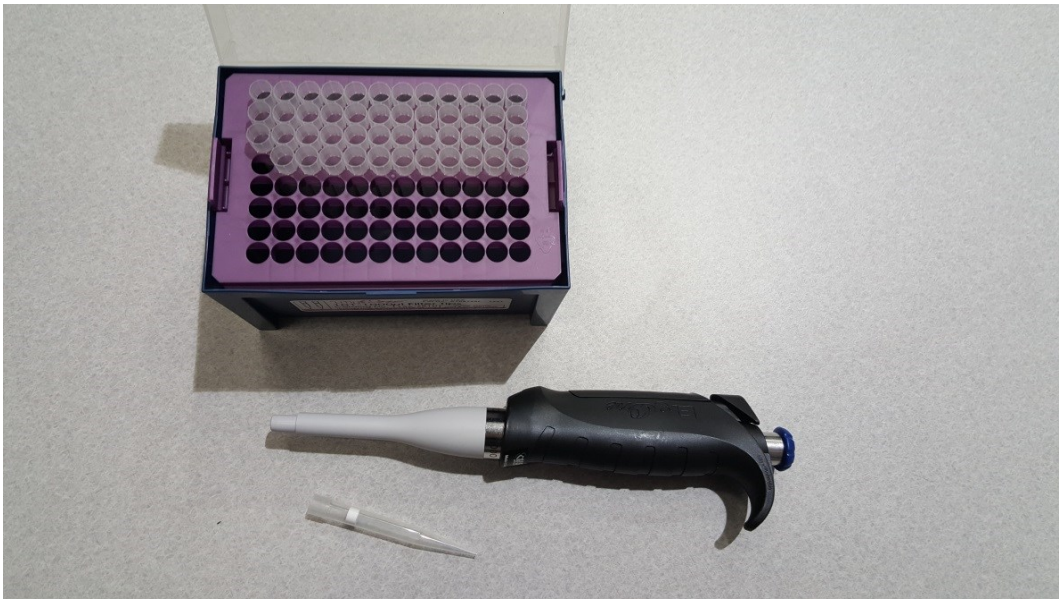

Figure 6: A micropipette and micropipette tips

Measurement Instruments

The accuracy of the miter saw was unknown, so an angle finder with a precision of +/- 0.5° was used to measure the true angle of each clipboard inserted into each cut of the two-by-four, see **Table 1**. For simplicity, when discussing the experimental apparatus, this thesis will use the value of the "Theoretical Angle" which encompasses the range 10-90 degrees in 10-degree increments. However all the data was calculated using the "Actual Angle" of the setup which is the same as the AOI.

Table 1: Theoretical vs Actual Angles in Drop apparatus

Theoretical Angle	Actual Angle
10	10
20	21
30	31
40	41
50	52
60	58
70	69
80	78
90	89

Digital calipers with a precision of +/-0.005mm were used to measure the length and width of the stain and a drafting divider was used to determine the points at which to measure the length of the stain. These dividers have little inherent error aside from that due to user technique. Finally, an inch-scale tape measure was used to find the height above ground for the drop point with a precision of +/- 1/32in. See **Figure 7**.

Figure 7: Measurement Tools

Data Collection

After applying the possible variables to the statistical software G*Power, the appropriate number of sample drops needed for each angle was found to be twelve. Using a 0.5ml micropipette, blood was dropped at 90 degrees to the ground from a known height of 84.1375cm (converted from 33 1/8" on the tape measure) onto a clipboard holding the control. Drops were deposited on the clipboard at each known angle ranging from 10 to 90 degrees in 10-degree increments, again see **Table 1**. This same approach was used for each of the sample fabrics. A total of three hundred and twenty-four stains were collected.

Once the control and fabric swatches were dry, digital calipers and a drafting divider were used to take measurements of the length and width of the stains using the right triangle analogy shown in **Figure 8**.

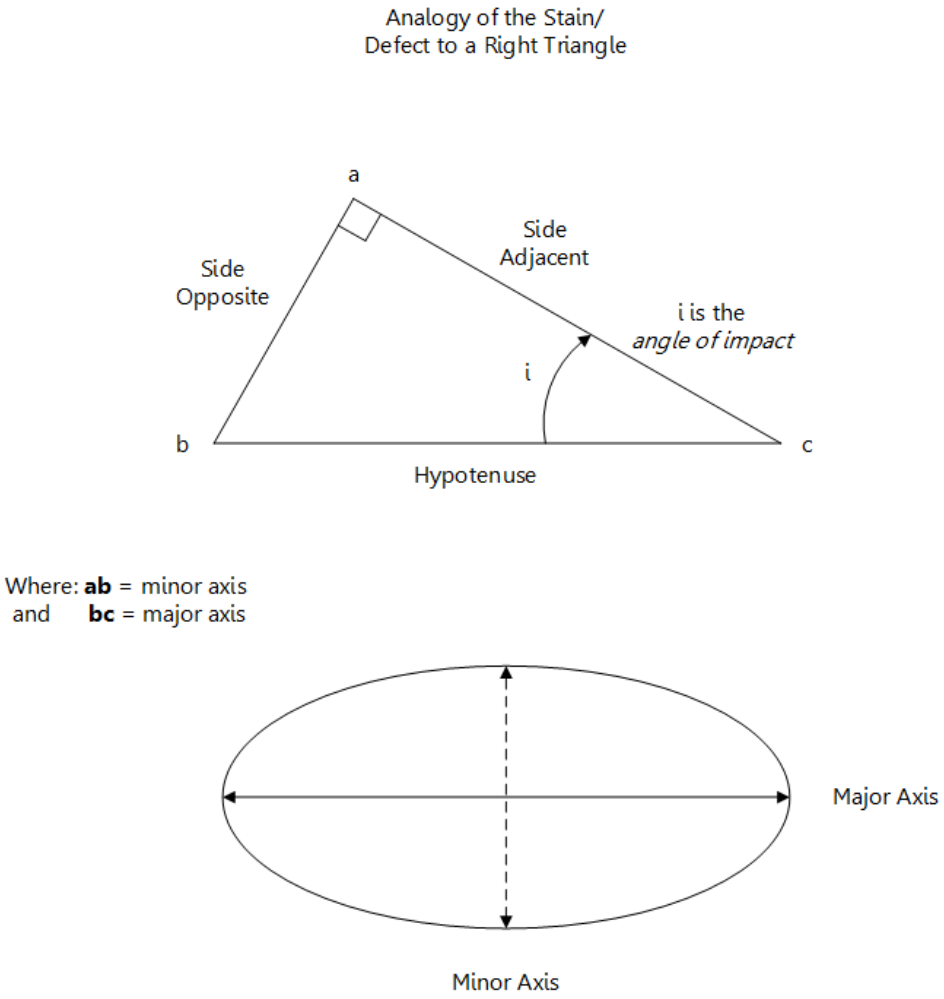

Figure 8: Right Triangle Analogy

To measure the length and width necessary to calculate the AOI, the model from **Figure 8** was applied to an actual bloodstain on a smooth, non-porous surface as shown in **Figure 10**. Note that the distortion from the terminal edge, or "tail", is excluded from the elliptical overlay and that the top of the stain, which is asymmetrical, is also excluded. This analogous

methodology of applying a perfect geometrical shape to an imperfect bloodstain is considered a source of systematic error and lends itself to the relatively large range for AOI or area of origin calculations that is acceptable. The skill of the technician making the measurements can help to reduce this error to a repeatable minimum.

The divider was used to eliminate the distortion by measuring the widest part of the drop then transferring that distance from the center of the minor axis to leading edge. Doubling the transferred distance gives the length of the major axis which can be marked off by rotating the divider to the terminal edge (James, Kish, & Sutton, 2005).

The AOI, shown in **Figure 9** , was calculated for each drop using the formula:

$$Impact\ angle = \sin^{-1}\left(\frac{Width}{Length}\right) \qquad \textbf{(Eq. 1)}$$

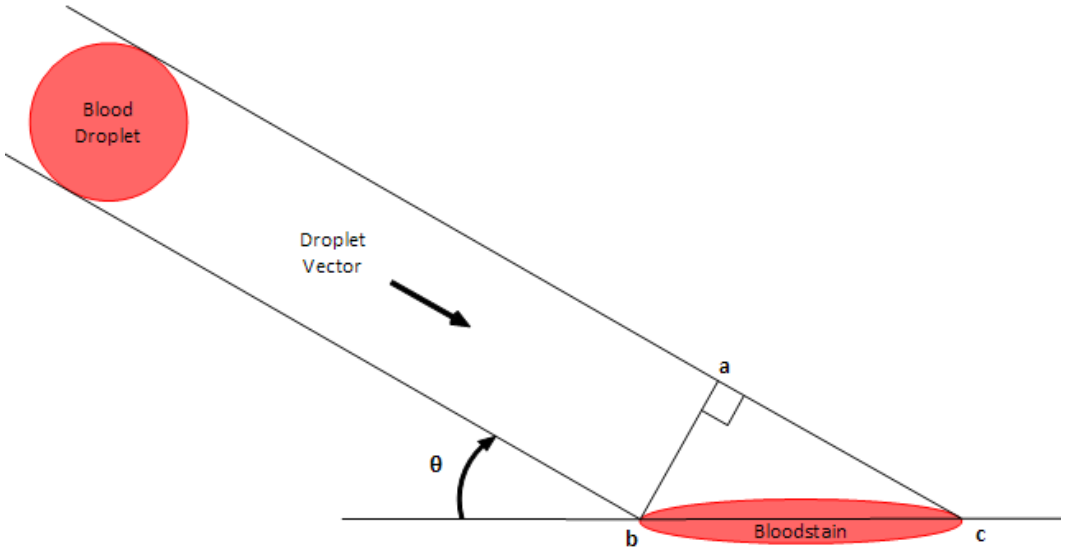

Figure 9: Angle of Impact (θ)

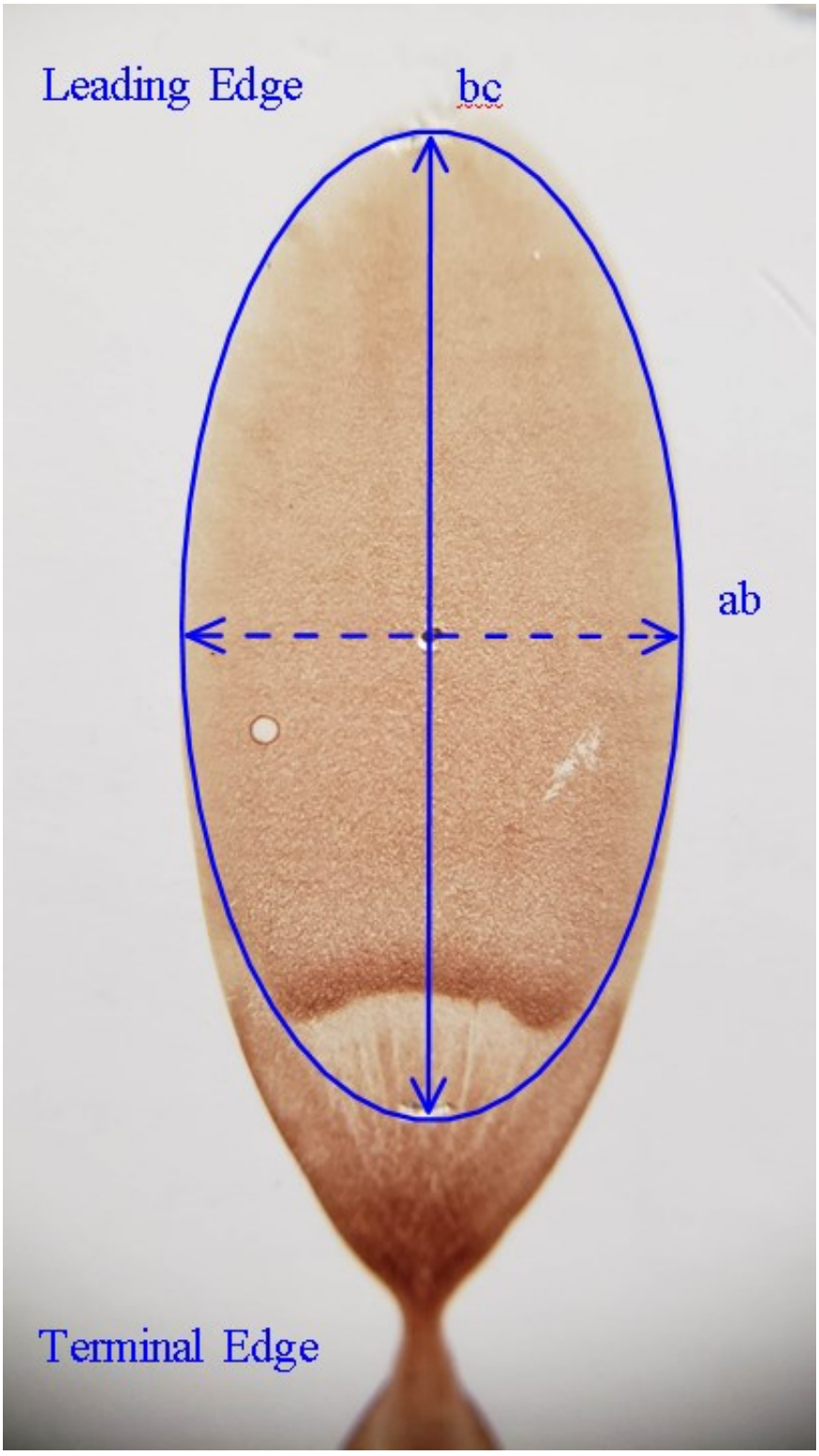

Figure 10: Anatomy of a Bloodstain

AOI Error Calculation

To account for random errors in the AOI calculations from **Eq. 1**, a propagation of error calculation was performed, using **Eq. 2**. The resulting error can be found with the raw data in **Appendix A** – **Appendix C**. Where the width and length are equal, **Eq. 2** fails and "N/A" appears in the tables. The maximum error of any calculated AOI was 1.83 x10^{-2} degrees.

$$\boldsymbol{\Delta f(w,l)} = \sqrt{\left(\frac{\partial f}{\partial w}\boldsymbol{\Delta w}\right)^2 + \left(\frac{\partial f}{\partial l}\boldsymbol{\Delta l}\right)^2}$$

$$= \sqrt{\left(\frac{\boldsymbol{\Delta w}}{l\sqrt{1-\frac{w^2}{l^2}}}\right)^2 + \left(\frac{(-\mathbf{w})\boldsymbol{\Delta l}}{l^2\sqrt{1-\frac{w^2}{l^2}}}\right)^2} \qquad \textbf{(Eq. 2)}$$

$f(w,l) = Impact\ Angle$ (**Eq. 1**), degrees
$\boldsymbol{\Delta} f = Impact\ Angle\ error$, degrees
$w, l = width\ \&\ length$, mm
$\boldsymbol{\Delta} w, \boldsymbol{\Delta} l = width\ \&\ length\ error$, mm

Statistical Data Analysis

To look for statistical relations in the collected data, the absolute value of the difference between the calculated angle and the measured angle was computed for each of the 324 drops. An analysis of covariance (ANCOVA) for the data was then performed with a main effect for type of surface and a covariate for the actual angle. The ANCOVA tests for differences between the mean absolute differences of the angles with respect to type of surface and actual angle. This analysis was followed by Tukey's multiple comparisons when appropriate.

Collected Bloodstains

Photos of collected bloodstains are shown in **Appendix D - Appendix F**, see **Figure 11** for scale details. To minimize glare, an 11" x 14" polycarbonate plate was placed on top of the

sample surface, texture side up (see **Figure 12**). This was used as a surface to clearly label each stain A-L corresponding to the order in which they were measured and recorded. Each stain was labeled in pencil when they were created to prevent ink bleed from corrupting the stain.

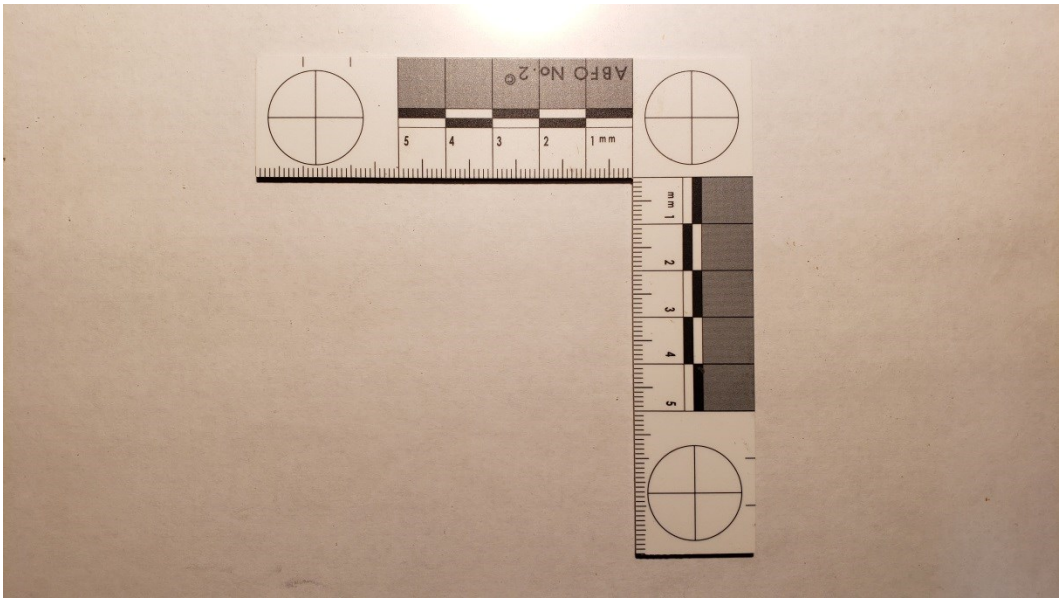

Figure 11: Scale used in Bloodstain Images

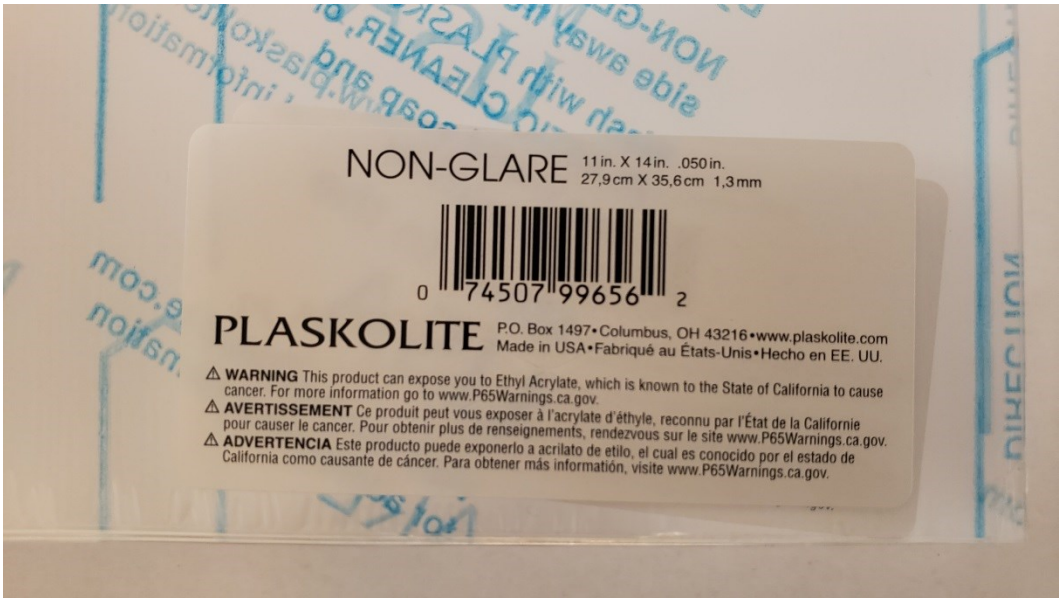

Figure 12: Bloodstain Image Cover Plate

Chapter Four: *Results*

Introduction

The primary research objective of this thesis was to determine if the mathematical equations used to measure the AOI on a smooth, non-porous surface in a bloodshed event can provide acceptable results when applied to bloodstains on non-smooth, porous fabric. A Control was used to validate the experimental design and two fabrics were used to test the thesis using the procedure described in the Methods section.

The results showed that for each of the non-smooth, porous fabrics, the AOI calculated from the bloodstains meets the acceptability criteria of +/- 5° compared to the actual AOI set by the experimental apparatus.

Statistical Analysis of Data

A statistical analysis was applied to the absolute value of the difference between the calculated angle and the actual angle to determine if a significant interaction could be observed between surface and AOI. For each measurement (12 data points for each angle were tested on each of the 3 surfaces for a total of 324 data points), calculations were as follows: the absolute difference between the calculated and actual angle, the mean of the difference, the standard deviation, and the minimum and maximum difference for the sets of data for each angle from 10-90 degrees. The statistical summary is shown in **Table 2** while the raw data (to include the absolute difference calculations) is available in **Appendix A – Appendix C**.

Table 2: Statistical Summary

Theoretical Angle (Actual)	Surface	Mean Difference	Standard Deviation	Min Difference (per angle)	Max Difference (per angle)
10	Control	0.85	0.48	0.03	1.44
(10)	1F	1.06	0.65	0.14	2.15
	2F	0.88	0.68	0.05	1.92
20	Control	0.99	0.58	0.08	1.93
(21)	1F	1.88	1.02	0.61	3.69
	2F	0.87	0.88	0.09	2.85
30	Control	0.94	0.64	0.17	2.42
(31)	1F	0.85	1.02	0.02	3.14
	2F	1.11	0.87	0.18	2.72
40	Control	1.31	0.71	0.21	2.32
(41)	1F	1.20	0.93	0.16	2.71
	2F	0.83	0.63	0.12	1.88
50	Control	1.52	1.00	0.25	3.17
(52)	1F	0.92	0.81	0.10	2.64
	2F	1.70	1.24	0.26	3.51
60	Control	1.60	1.03	0.12	4.14
(58)	1F	2.65	1.49	0.23	4.46
	2F	0.95	0.77	0.31	3.04
70	Control	1.16	0.52	0.25	1.85
(69)	1F	2.19	1.36	0.78	4.66
	2F	1.18	0.69	0.18	2.14
80	Control	1.27	1.30	0.05	3.44
(78)	1F	1.42	0.78	0.42	2.97
	2F	1.36	0.81	0.42	3.25
90	Control	1.06	0.10	1.00	1.23
(89)	1F	1.67	0.72	1.00	2.82
	2F	2.01	1.00	1.00	3.98

Table 3: Overall difference ranges for each surface tested

	Minimum Difference	Maximum Difference
Control	0.03	4.14
1F	0.02	4.66
2F	0.05	3.98

Table 2 shows the minimum and maximum difference values, by angle, for each surface giving the range that the individual data points fall into. This illustrates the results of this thesis by directly showing that the calculated angles for the Control as well as both Fabrics fall within the acceptability criteria of +/- 5° (between 0 and 5 for the absolute difference used herein). The overall difference ranges for each surface are shown in **Table 3**.

There was no significant interaction between type of surface and the actual angle ($F = 0.94$, $p = 0.393$); consequently, the interaction term was removed from the analysis and the surface was analyzed independently.

The type of surface effect of this experiment compared the mean absolute differences for the three surfaces (each fabric and the Control). This effect was found to be statistically significant ($F = 23.95$, $p < 0.001$). The mean of the absolute value of the differences for Fabric 1 was found to be significantly greater than the means for the Control surface ($t = 2.75$, $p = 0.017$) and Fabric 2 ($t = 2.57$, $p = 0.029$)), see **Figure 13**. There are no other significant differences. The estimated mean difference between fabric 1 and the control surface is only 0.35°, and the estimated mean difference between fabric 1 and fabric 2 is only 0.33°. While this result is *statistically* significant, it is not *practically* significant due to the fact that the accepted difference between measured and actual AOIs is large (+/- 5°).

Figure 14 shows the individual data points used to calculate the absolute mean difference for the Control material. From this plot it can be seen that while some of the data points are relatively far from the mean line, all data points are still well within the accepted range for calculated AOIs. **Figure 15** and **Figure 16** similarly show this for Fabric 1 and Fabric 2.

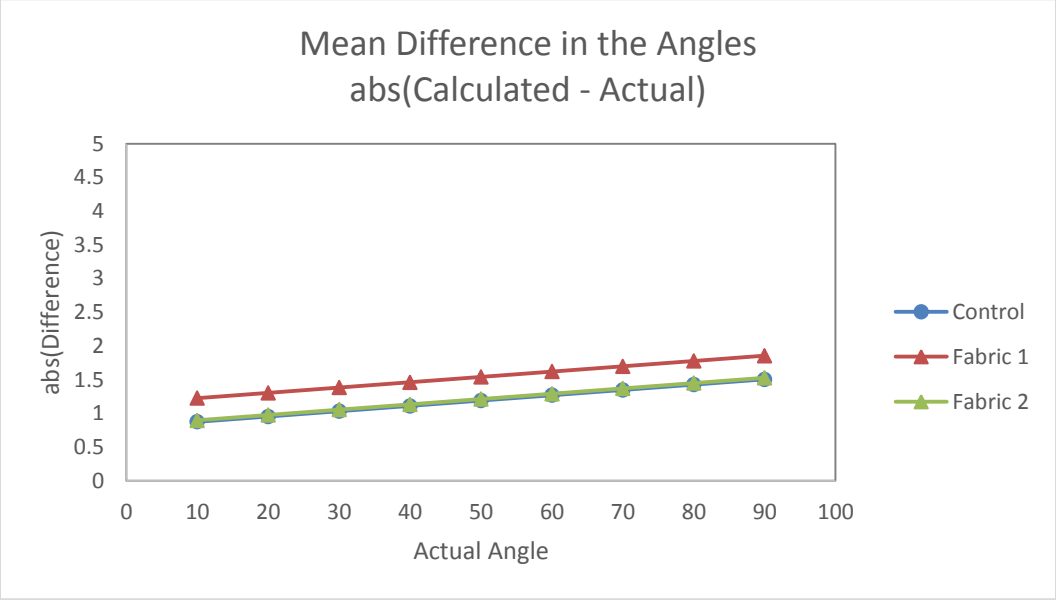

Figure 13: Comparison of Mean Differences for Each Surface

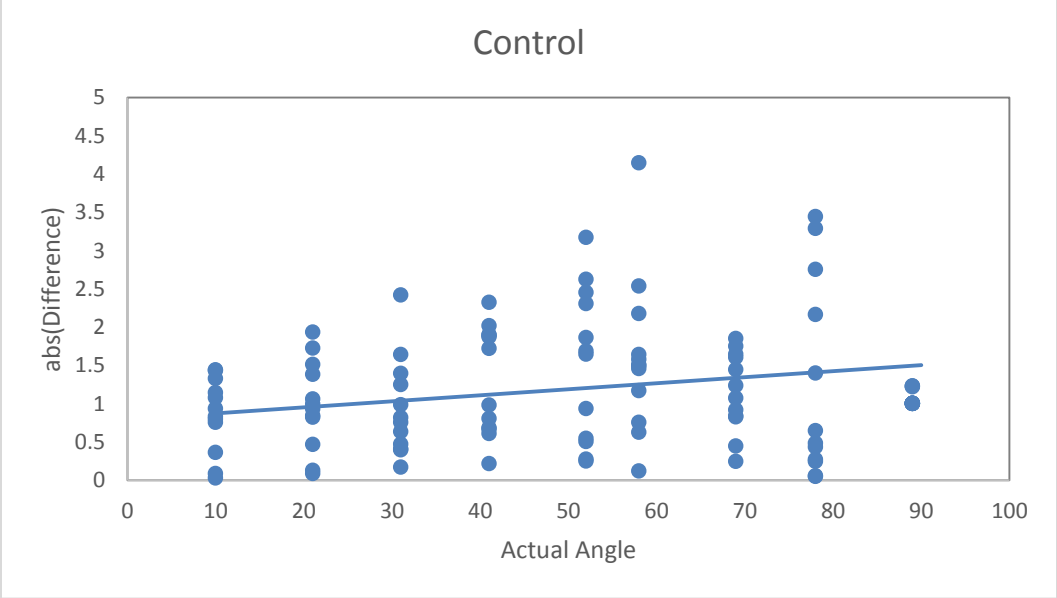

Figure 14: Absolute Difference of Calculated and Actual Angles vs. Actual Angles, Control

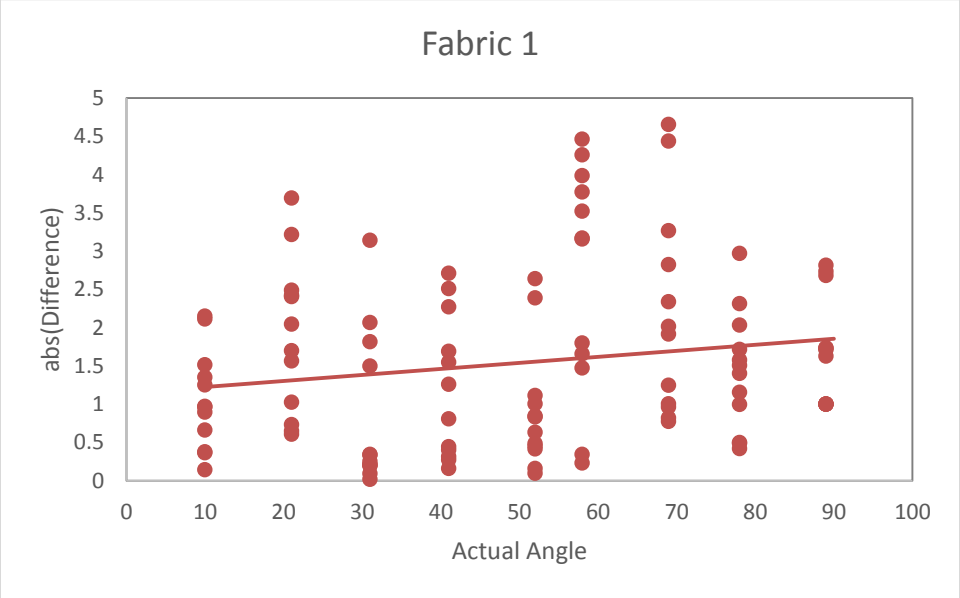

Figure 15: Absolute Difference of Calculated and Actual Angles vs. Actual Angles, Fabric 1

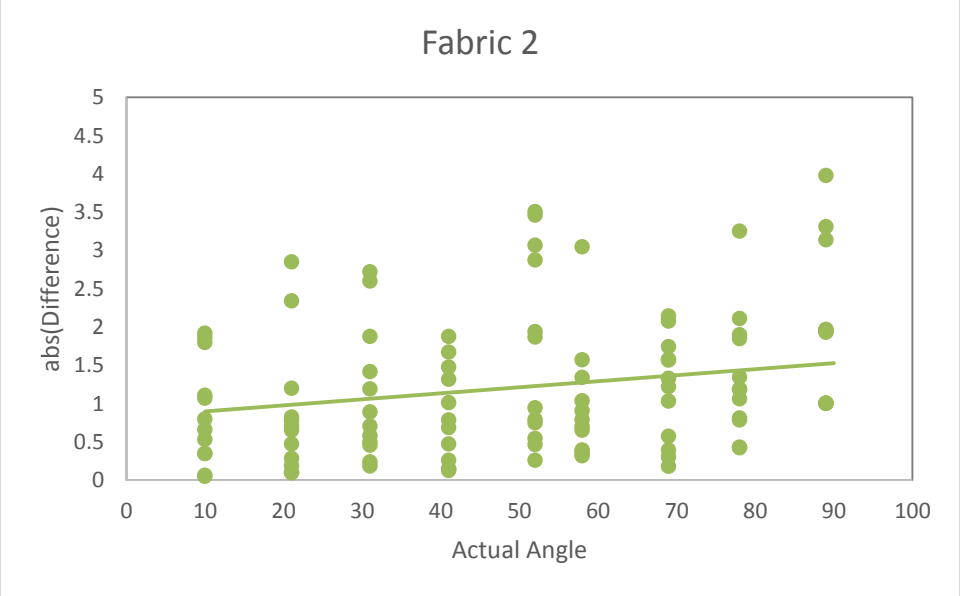

Figure 16: Absolute Difference of Calculated and Actual Angles vs. Actual Angles, Fabric 2

Chapter Five: *Discussion*

Introduction

After a bloodshed event, a bloodstain analyst uses their knowledge of blood droplet mechanics, both in-flight and upon impact to a surface, to help determine the sequence of events that occurred. The bloodstain evidence found at a crime scene must be compared to known methodologies that yield consistent and reproducible results, methodologies that are currently limited to bloodstain research conducted on smooth, non-porous surfaces. Because of this, unknown stains at a crime scene that are useable for analysis are limited to these surfaces which can reduce the effectiveness of the evidence.

In order for analysts and investigators to have the best chance to recreate events accurately, the ability to utilize the maximum amount of available blood evidence is critical. Limiting that evidence to only that which is collected from smooth, non-porous surfaces is a major issue that is due mainly to lack of existing research into the viability of other materials that bloodstain evidence can be harvested from, specifically fabrics. It is imperative that the field of forensic science continues to push forward on research on, and expand training in, the collection and analysis of bloodstains collected from surfaces other than those currently accepted as reliable.

In order to advance the necessary research data, it must be determined if the existing mathematical principles used to determine the AOI of blood spatter evidence deposited on smooth, non-porous surfaces can reliably be applied to blood evidence on non-smooth, porous surfaces as well. The results of this thesis show evidence that, at least for the fabrics tested, this advancement looks promising.

Discussion

The statistical analysis compared all three trials (Control, Fabric 1 and Fabric 2) to each other to look for significant differences in the data. Because this work was only interested in whether or not the calculated angle was within the accepted range, the absolute value of the difference between the calculated and the actual angle was used in the ANCOVA test to look for interactions between the surface material and each tested angle. The test showed no significant interaction between them ($F = 0.94$, $p = 0.393$) so the material and angle could be looked at independently.

Looking at the surfaces independent of angle (via Tukey's test), the difference between calculated and actual AOIs for Fabric 1 ($F = 23.95$, $p < 0.001$) showed statistically significant differences from both Fabric 2 and the Control for all angles tested, see **Figure 13**. The Control and Fabric 2 were nearly identical to each other with test values of ($t = 2.75$, $p = 0.017$) and ($t = 2.57$, $p = 0.029$), respectively. Looking at the actual differences in the means, Fabric 1 was 0.35° different from the Control and 0.33° different from Fabric 2 showing statistically significant results that are irrelevant when you consider the large acceptable range for the calculated AOI vs actual AOI while the difference between the Control and Fabric 2 was only 0.02°.

While the differences in the means for each material were *statistically* significant, this was not *practically* significant. The reason for the difference seen in **Figure 13** between Fabric 1 and the other two materials is undetermined (possibly due to fabric construction) but is shown to be irrelevant as the differences were only approximately 3.5% of the accepted calculated AOI range of 10°.

This thesis was successful in that there was no difference between the measured and actual AOI on each fabric due to wicking greater than the acceptable variance of +/- 5° satisfying the primary research objective of determining if the mathematical equations used to measure the AOI on a smooth, non-porous surface can provide acceptable results when applied to bloodstains on non-smooth, porous fabric in a bloodshed event. Furthermore, the Control surface's measured angles yielded acceptable results which show that the experimental design used in this thesis is suited for future research into additional fabrics.

The results of this thesis show that bloodstains documented from 100% cotton fabric and 98% cotton and 2% spandex fabric can be analyzed using the same mathematical model as bloodstains documented from smooth, non-porous surfaces. This is significant to the field of forensic science in that, with further research, future bloodstain pattern analysts will have a larger data pool from which to document evidence at a crime scene. The limitations of this study, namely limited fabric types and constructs tested, will also provide future researchers opportunities to expand upon the results of this thesis. This could prove invaluable for the field of BPA in the future.

Limitations

This project used pork blood from a local butchery to eliminate any effects anticoagulants might have on the wicking process. Once outside the body, blood is affected by environmental conditions and as time passes, the blood will clot and become unusable. The blood used in this experiment was stirred continuously to inhibit the clotting factor and a new source of pork blood was collected for each sample set tested.

This project was done in a laboratory setting where the environment was controlled. At a crime scene, blood evidence must be collected from an area or object that has some permanency or documented with photographs well enough to replicate the scene. A fitted sheet on a bed is less likely to be altered than a pillow that can be easily moved or curtains that can be moved by air flow. Good documentation is vital when looking for a pattern and area of convergence.

Droplets on smooth, non-porous surfaces may contain features such as spines and tails. These features are not included in the length and width, and it is generally the decision of a bloodstain analyst what portion of a stain is to be measured. Droplets on porous surfaces, such as fabrics, have less distinguishing spine and tail features due to the wicking factor and require a higher skill level to determine what portion needs to be measured.

This study could not test all the possible combinations of fabric construction and composition. Fabric type and construct can affect how blood interacts with fabric. Each fiber type and construct needs to be examined individually against a control to build a pool of reproducible data.

The biggest limitation in any BPA research is the researcher. The AOI in this study was found by manually measuring droplets with calipers. Depending on the skill level and work experience of future analysts, the results could differ from analyst to analyst. This potential problem is solved by understanding that the point of origin is actually an area and that the acceptable range of error is +/- 5°.

Future Research

Concerns about whether the laundering of fabrics would affect the AOI results calculated from those fabrics were shown to not be a factor for the materials tested as they were laundered

before the experiment according to the procedure outlined in the **Intervention and Materials** section. Additionally, even with constant stirring, the clotting of un-treated blood was considered a possible source of systematic error that could affect the wicking of bloodstains incident on the tested fabrics but did not appear to affect the results of this work.

While this thesis was necessarily limited in scope, it is a promising starting point for future research which can address the limitations of this work. As this project was the first of its kind, it served to identify experimental variables and isolate many different sources of error (both systematic and procedural) that can be focused on in additional testing to better define the viability of applying accepted mathematical processes for smooth, non-porous materials to non-smooth, porous materials. Suggested topics of future research are:

1. Digital vs Manual data collection. This thesis utilized manual measurement methods but there are computer programs that can determine the AOI from images. However, research using digital methods is still experimental and requires the oversight of an experienced analyst and, as in this thesis, the analyst's experience can be a source of error.

2. Additional Fabric types. This thesis only tested two commonly found fabrics and therefore cannot speak for other fabric types and constructs. Additional research is needed to determine if other fabrics can produce similar results to this work in an effort to build experimental data to support their use in crime scene investigation.
3. The effect of detergents and dyes on wicking. This is a very complex research goal as a fabric would first need to be shown to produce acceptable AOI calculations using the methods in this thesis and then the research would need to verify the effects of

selected detergents on that fabric. Additionally, the same fabric type in different colors (or type of dye) would also need to be assessed.

Conclusion

While qualitative comparisons of bloodstains are useful for determining the *type* of blood evidence, it is not the correct way to determine the validity of bloodstain evidence found on fabric for use in AOI calculations. Inspection of **Eq. 1** shows the only relevant variable in the calculation of AOI is the width/length ratio of the bloodstain, a quantitative property. The fabrics tested in this thesis have a proportional wicking factor that maintained width/length ratio and yielded an accurate AOI calculation. It should be expected that future research in other non-smooth, porous materials with similar wicking properties would also yield acceptable results.

By continuing this successful research to validate additional fabrics and other porous surfaces, the bloodstain samples an analyst can use from a bloodshed event become less limited. Currently, samples used have to be found on smooth, nonporous surfaces, but if wicking has no effect on the calculated range found for the point of origin, then samples found on fabrics can also be used as evidence.

This thesis is of great importance to the forensic science field of BPA as it can help update the stagnant practices of bloodstain evidence collection to a more inclusive model and enable the analyst much more flexibility. The currently accepted method of BPA using the right triangle analogy is applicable to the two fabrics tested in this work, and in the future with further validation, should be considered viable blood evidence sources.

References

Balthazard, V. et al. (1939). Etude des Gouttes de Sang Projecte. Presented at *XXII Congress de Medicine Legale*. Paris.

Bevel, T., & Gardner, R. M. (1990). Bloodstain Pattern Analysis: Theory and Practice—A Laboratory Manual. *TBI Inc., Oklahoma City, OK*, 38.

Gardner, R. M. (2012). *Practical Crime Scene Processing and Investigation* (2nd ed.). Boca Raton, FL: CRC Press Taylor & Francis Group.

Holbrook, M. (2010). RESEARCH ARTICLE: Evaluation of Blood Deposition on Fabric: Distinguishing Spatter and Transfer Stains. *International Association of Bloodstain Pattern Analysts News*, *26*(1), 3–12. Retrieved from http://www.iabpa.org/uploads/files/iabpa publications/March 2010 News.pdf

James, S. H., Kish, P. E., & Sutton, T. P. (2005). *Principles of bloodstain pattern analysis: theory and practice*. CRC Press.

MacDonell, H. (1982). *Bloodstain Pattern Interpretation*. New York: Laboratory of Forensic Science.

Metcalf, H. J. (1980). *Topics in Classical Bio-Physics*. NJ: Prentice Hall.

Organization of Scientific Area Committees for Forensic Science. (2017). Terms and definitions in bloodstain pattern analysis. ASB Technical Report 033.

Reynolds, M., & Silenieks, E. (2016). Consideration for the Assessment of Bloodstains on Fabrics. *Journal of Bloodstain Pattern Analysis*, *32*(2), 15–20. Retrieved from http://www.iabpa.org/uploads/files/iabpa publications/December 2016 JBPA.pdf

Appendix A – Raw Data (Control)

Type	Sample ID	Width (mm)	Length (mm)	Calculated Angle (deg)	Error Propagation (+/- deg)	Actual Angle (deg)	Absolute Difference (deg)
Control	C_90_a	13.33	13.33	90.00	N/A	89	1.00
Control	C_90_b	13.29	13.29	90.00	N/A	89	1.00
Control	C_90_c	13.53	13.53	90.00	N/A	89	1.00
Control	C_90_d	12.82	12.82	90.00	N/A	89	1.00
Control	C_90_e	13.32	13.33	87.78	1.37E-02	89	1.22
Control	C_90_f	13.26	13.26	90.00	N/A	89	1.00
Control	C_90_g	12.67	12.67	90.00	N/A	89	1.00
Control	C_90_h	13.38	13.38	90.00	N/A	89	1.00
Control	C_90_i	13.15	13.15	90.00	N/A	89	1.00
Control	C_90_j	13.21	13.22	87.77	1.37E-02	89	1.23
Control	C_90_k	13.35	13.35	90.00	N/A	89	1.00
Control	C_90_l	13.16	13.17	87.77	1.38E-02	89	1.23
Control	C_80_a	12.76	13.16	75.84	2.20E-03	78	2.16
Control	C_80_b	12.85	13.00	81.29	3.59E-03	78	3.29
Control	C_80_c	12.87	13.19	77.35	2.45E-03	78	0.65
Control	C_80_d	12.83	13.13	77.73	2.54E-03	78	0.27
Control	C_80_e	12.55	13.02	74.56	2.04E-03	78	3.44
Control	C_80_f	12.60	12.87	78.24	2.70E-03	78	0.24
Control	C_80_g	12.61	13.04	75.25	2.13E-03	78	2.75
Control	C_80_h	12.88	13.17	77.95	2.57E-03	78	0.05
Control	C_80_i	12.91	13.22	77.57	2.49E-03	78	0.43
Control	C_80_j	12.80	13.11	77.52	2.47E-03	78	0.48
Control	C_80_k	12.67	12.89	79.40	2.96E-03	78	1.40
Control	C_80_l	12.86	13.15	77.94	2.55E-03	78	0.06
Control	C_70_a	12.65	13.51	69.45	1.44E-03	69	0.45
Control	C_70_b	12.63	13.39	70.60	1.55E-03	69	1.60
Control	C_70_c	12.46	13.19	70.85	1.59E-03	69	1.85
Control	C_70_d	12.72	13.53	70.07	1.49E-03	69	1.07
Control	C_70_e	11.96	12.79	69.25	1.51E-03	69	0.25
Control	C_70_f	12.70	13.53	69.83	1.47E-03	69	0.83
Control	C_70_g	12.52	13.27	70.64	1.56E-03	69	1.64
Control	C_70_h	11.95	12.73	69.84	1.56E-03	69	0.84
Control	C_70_i	12.74	13.52	70.44	1.52E-03	69	1.44
Control	C_70_j	12.14	12.90	70.23	1.57E-03	69	1.23
Control	C_70_k	12.82	13.65	69.92	1.46E-03	69	0.92
Control	C_70_l	11.99	12.70	70.75	1.64E-03	69	1.75

Type	Sample ID	Width (mm)	Length (mm)	Calculated Angle (deg)	Error Propagation (+/- deg)	Actual Angle (deg)	Absolute Difference (deg)
Control	C_60_a	12.15	14.10	59.51	9.23E-04	58	1.51
Control	C_60_b	11.79	13.59	60.18	9.79E-04	58	2.18
Control	C_60_c	12.49	14.83	57.37	8.18E-04	58	0.63
Control	C_60_d	11.92	14.24	56.83	8.37E-04	58	1.17
Control	C_60_e	12.04	13.98	59.46	9.29E-04	58	1.46
Control	C_60_f	11.65	13.51	59.58	9.65E-04	58	1.58
Control	C_60_g	11.64	13.51	59.49	9.62E-04	58	1.49
Control	C_60_h	11.51	13.22	60.53	1.02E-03	58	2.53
Control	C_60_i	12.27	14.59	57.24	8.28E-04	58	0.76
Control	C_60_j	12.46	14.44	59.64	9.05E-04	58	1.64
Control	C_60_k	11.82	13.92	58.12	8.92E-04	58	0.12
Control	C_60_l	11.75	13.29	62.14	1.07E-03	58	4.14
Control	C_50_a	11.02	14.32	50.31	6.90E-04	52	1.69
Control	C_50_b	11.57	15.37	48.83	6.19E-04	52	3.17
Control	C_50_c	11.59	15.27	49.38	6.31E-04	52	2.62
Control	C_50_d	12.12	15.74	50.36	6.28E-04	52	1.64
Control	C_50_e	11.88	15.19	51.45	6.71E-04	52	0.55
Control	C_50_f	12.08	15.84	49.70	6.14E-04	52	2.30
Control	C_50_g	11.95	15.27	51.50	6.68E-04	52	0.50
Control	C_50_h	11.36	14.47	51.73	7.09E-04	52	0.27
Control	C_50_i	12.00	15.28	51.75	6.72E-04	52	0.25
Control	C_50_j	11.73	15.08	51.06	6.68E-04	52	0.94
Control	C_50_k	11.65	15.31	49.55	6.33E-04	52	2.45
Control	C_50_l	11.56	15.06	50.14	6.53E-04	52	1.86
Control	C_40_a	10.52	16.68	39.10	4.57E-04	41	1.90
Control	C_40_b	10.78	17.09	39.11	4.46E-04	41	1.89
Control	C_40_c	10.87	17.17	39.28	4.45E-04	41	1.72
Control	C_40_d	11.03	17.65	38.68	4.28E-04	41	2.32
Control	C_40_e	10.74	16.60	40.31	4.70E-04	41	0.69
Control	C_40_f	10.88	16.79	40.39	4.66E-04	41	0.61
Control	C_40_g	10.79	16.78	40.02	4.63E-04	41	0.98
Control	C_40_h	10.92	16.92	40.19	4.60E-04	41	0.81
Control	C_40_i	10.81	16.26	41.67	4.94E-04	41	0.67
Control	C_40_j	10.82	17.20	38.98	4.42E-04	41	2.02
Control	C_40_k	10.87	16.64	40.79	4.74E-04	41	0.21
Control	C_40_l	11.05	17.51	39.13	4.35E-04	41	1.87

Type	Sample ID	Width (mm)	Length (mm)	Calculated Angle (deg)	Error Propagation (+/- deg)	Actual Angle (deg)	Absolute Difference (deg)
Control	C_30_a	9.98	20.11	29.75	3.20E-04	31	1.25
Control	C_30_b	9.94	19.87	30.02	3.25E-04	31	0.98
Control	C_30_c	9.58	19.02	30.24	3.41E-04	31	0.76
Control	C_30_d	9.61	19.60	29.36	3.26E-04	31	1.64
Control	C_30_e	9.64	18.81	30.83	3.48E-04	31	0.17
Control	C_30_f	9.19	19.21	28.58	3.29E-04	31	2.42
Control	C_30_g	9.62	19.03	30.37	3.41E-04	31	0.63
Control	C_30_h	9.52	18.74	30.53	3.47E-04	31	0.47
Control	C_30_i	9.97	18.91	31.82	3.52E-04	31	0.82
Control	C_30_j	9.49	18.21	31.41	3.63E-04	31	0.41
Control	C_30_k	9.58	18.39	31.40	3.59E-04	31	0.40
Control	C_30_l	9.56	19.35	29.61	3.31E-04	31	1.39
Control	C_20_a	7.79	22.70	20.07	2.48E-04	21	0.93
Control	C_20_b	7.84	22.75	20.16	2.48E-04	21	0.84
Control	C_20_c	7.50	22.34	19.62	2.51E-04	21	1.38
Control	C_20_d	7.68	23.51	19.07	2.37E-04	21	1.93
Control	C_20_e	7.61	21.36	20.87	2.66E-04	21	0.13
Control	C_20_f	7.79	22.77	20.01	2.47E-04	21	0.99
Control	C_20_g	8.13	22.60	21.08	2.52E-04	21	0.08
Control	C_20_h	7.58	22.96	19.28	2.43E-04	21	1.72
Control	C_20_i	7.83	22.96	19.94	2.45E-04	21	1.06
Control	C_20_j	7.93	21.67	21.47	2.64E-04	21	0.47
Control	C_20_k	8.14	23.60	20.18	2.39E-04	21	0.82
Control	C_20_l	7.95	23.83	19.49	2.35E-04	21	1.51
Control	C_10_a	5.17	30.88	9.64	1.67E-04	10	0.36
Control	C_10_b	5.45	31.12	10.09	1.66E-04	10	0.09
Control	C_10_c	5.47	28.84	10.93	1.80E-04	10	0.93
Control	C_10_d	5.00	28.87	9.97	1.78E-04	10	0.03
Control	C_10_e	5.46	29.26	10.75	1.77E-04	10	0.75
Control	C_10_f	5.73	30.59	10.80	1.69E-04	10	0.80
Control	C_10_g	5.61	28.28	11.44	1.84E-04	10	1.44
Control	C_10_h	5.64	28.71	11.33	1.81E-04	10	1.33
Control	C_10_i	5.57	29.65	10.83	1.75E-04	10	0.83
Control	C_10_j	5.74	29.88	11.08	1.74E-04	10	1.08
Control	C_10_k	5.77	29.86	11.14	1.74E-04	10	1.14
Control	C_10_l	5.86	29.57	11.43	1.76E-04	10	1.43

Appendix B – Raw Data (Fabric 1)

Type	Sample ID	Width (mm)	Length (mm)	Calculated Angle (deg)	Error Propagation (+/- deg)	Actual Angle (deg)	Absolute Difference (deg)
1F	1F_90_a	9.00	9.02	86.18	1.18E-02	89	2.82
1F	1F_90_b	9.40	9.42	86.27	1.15E-02	89	2.73
1F	1F_90_c	8.76	8.77	87.26	1.69E-02	89	1.74
1F	1F_90_d	9.50	9.51	87.37	1.62E-02	89	1.63
1F	1F_90_e	8.93	8.94	87.29	1.67E-02	89	1.71
1F	1F_90_f	8.62	8.62	90.00	N/A	89	1.00
1F	1F_90_g	9.02	9.02	90.00	N/A	89	1.00
1F	1F_90_h	9.25	9.25	90.00	N/A	89	1.00
1F	1F_90_i	9.67	9.69	86.32	1.14E-02	89	2.68
1F	1F_90_j	8.79	8.80	87.27	1.69E-02	89	1.73
1F	1F_90_k	9.24	9.24	90.00	N/A	89	1.00
1F	1F_90_l	8.88	8.88	90.00	N/A	89	1.00
1F	1F_80_a	9.22	9.38	79.40	4.10E-03	78	1.40
1F	1F_80_b	9.56	9.68	80.97	4.65E-03	78	2.97
1F	1F_80_c	9.35	9.52	79.16	3.95E-03	78	1.16
1F	1F_80_d	9.68	9.82	80.31	4.28E-03	78	2.31
1F	1F_80_e	9.19	9.34	79.72	4.24E-03	78	1.72
1F	1F_80_f	9.51	9.76	77.00	3.22E-03	78	1.00
1F	1F_80_g	9.41	9.57	79.51	4.06E-03	78	1.51
1F	1F_80_h	9.76	9.96	78.50	3.56E-03	78	0.50
1F	1F_80_i	9.14	9.28	80.04	4.40E-03	78	2.04
1F	1F_80_j	9.54	9.70	79.58	4.00E-03	78	1.58
1F	1F_80_k	9.75	9.95	78.49	3.53E-03	78	0.49
1F	1F_80_l	9.60	9.83	77.58	3.31E-03	78	0.42
1F	1F_70_a	8.42	9.07	68.18	2.02E-03	69	0.82
1F	1F_70_b	8.95	9.42	71.82	2.35E-03	69	2.82
1F	1F_70_c	8.69	9.37	68.04	1.95E-03	69	0.96
1F	1F_70_d	9.11	9.81	68.22	1.87E-03	69	0.78
1F	1F_70_e	9.04	9.56	71.02	2.21E-03	69	2.02
1F	1F_70_f	8.29	8.75	71.34	2.46E-03	69	2.34
1F	1F_70_g	9.20	9.79	70.01	2.05E-03	69	1.01
1F	1F_70_h	9.50	9.90	73.66	2.49E-03	69	4.66
1F	1F_70_i	9.01	9.40	73.44	2.58E-03	69	4.44
1F	1F_70_j	8.60	9.10	70.92	2.31E-03	69	1.92
1F	1F_70_k	9.02	9.47	72.27	2.39E-03	69	3.27
1F	1F_70_l	9.20	9.94	67.75	1.81E-03	69	1.25

Type	Sample ID	Width (mm)	Length (mm)	Calculated Angle (deg)	Error Propagation (+/- deg)	Actual Angle (deg)	Absolute Difference (deg)
1F	1F_60_a	8.82	10.22	59.66	1.28E-03	58	1.66
1F	1F_60_b	8.70	9.83	62.26	1.46E-03	58	4.26
1F	1F_60_c	9.11	10.40	61.16	1.32E-03	58	3.16
1F	1F_60_d	9.26	10.51	61.77	1.34E-03	58	3.77
1F	1F_60_e	8.85	10.24	59.80	1.28E-03	58	1.80
1F	1F_60_f	8.74	9.90	61.99	1.43E-03	58	3.99
1F	1F_60_g	9.26	10.75	59.47	1.21E-03	58	1.47
1F	1F_60_h	9.00	10.15	62.46	1.42E-03	58	4.46
1F	1F_60_i	9.08	10.33	61.52	1.35E-03	58	3.52
1F	1F_60_j	9.42	11.15	57.66	1.10E-03	58	0.34
1F	1F_60_k	9.55	11.29	57.77	1.09E-03	58	0.23
1F	1F_60_l	9.12	10.41	61.17	1.32E-03	58	3.17
1F	1F_50_a	7.99	10.49	49.61	9.25E-04	52	2.39
1F	1F_50_b	8.67	10.88	52.83	9.73E-04	52	0.83
1F	1F_50_c	8.21	10.35	52.49	1.01E-03	52	0.49
1F	1F_50_d	8.42	10.62	52.45	9.86E-04	52	0.45
1F	1F_50_e	8.40	10.60	52.42	9.87E-04	52	0.42
1F	1F_50_f	8.10	10.40	51.16	9.72E-04	52	0.84
1F	1F_50_g	8.52	10.72	52.63	9.82E-04	52	0.63
1F	1F_50_h	8.72	11.09	51.84	9.28E-04	52	0.16
1F	1F_50_i	8.67	10.84	53.11	9.84E-04	52	1.11
1F	1F_50_j	8.46	10.75	51.90	9.59E-04	52	0.10
1F	1F_50_k	8.69	10.88	53.01	9.77E-04	52	1.01
1F	1F_50_l	8.18	10.78	49.36	8.94E-04	52	2.64
1F	1F_40_a	8.15	12.02	42.69	6.84E-04	41	1.69
1F	1F_40_b	8.32	12.57	41.44	6.36E-04	41	0.44
1F	1F_40_c	8.20	12.42	41.32	6.42E-04	41	0.32
1F	1F_40_d	8.14	11.78	43.71	7.14E-04	41	2.71
1F	1F_40_e	8.48	12.54	42.55	6.53E-04	41	1.55
1F	1F_40_f	8.09	12.03	42.26	6.77E-04	41	1.26
1F	1F_40_g	7.89	11.51	43.27	7.23E-04	41	2.27
1F	1F_40_h	7.89	11.46	43.51	7.30E-04	41	2.51
1F	1F_40_i	7.52	11.50	40.84	6.87E-04	41	0.16
1F	1F_40_j	8.02	12.03	41.81	6.70E-04	41	0.81
1F	1F_40_k	7.77	11.94	40.60	6.58E-04	41	0.40
1F	1F_40_l	8.41	12.89	40.73	6.11E-04	41	0.27

Type	Sample ID	Width (mm)	Length (mm)	Calculated Angle (deg)	Error Propagation (+/- deg)	Actual Angle (deg)	Absolute Difference (deg)
1F	1F_30_a	6.35	12.24	31.25	5.38E-04	31	0.25
1F	1F_30_b	7.15	13.89	30.98	4.72E-04	31	0.02
1F	1F_30_c	6.87	13.26	31.20	4.97E-04	31	0.20
1F	1F_30_d	6.79	13.11	31.19	5.02E-04	31	0.19
1F	1F_30_e	6.69	12.91	31.21	5.10E-04	31	0.21
1F	1F_30_f	6.49	12.08	32.50	5.57E-04	31	1.50
1F	1F_30_g	6.97	13.57	30.91	4.83E-04	31	0.09
1F	1F_30_h	6.36	13.61	27.86	4.59E-04	31	3.14
1F	1F_30_i	6.46	11.92	32.82	5.68E-04	31	1.82
1F	1F_30_j	6.22	11.40	33.07	5.96E-04	31	2.07
1F	1F_30_k	6.47	12.69	30.65	5.14E-04	31	0.35
1F	1F_30_l	6.74	12.96	31.34	5.09E-04	31	0.34
1F	1F_20_a	5.47	15.73	20.35	3.59E-04	21	0.65
1F	1F_20_b	6.12	14.92	24.22	3.97E-04	21	3.22
1F	1F_20_c	5.54	14.96	21.74	3.84E-04	21	0.74
1F	1F_20_d	5.87	15.21	22.70	3.82E-04	21	1.70
1F	1F_20_e	6.05	15.22	23.42	3.85E-04	21	2.42
1F	1F_20_f	5.90	15.07	23.05	3.87E-04	21	2.05
1F	1F_20_g	6.19	15.53	23.49	3.78E-04	21	2.49
1F	1F_20_h	6.09	16.24	22.02	3.55E-04	21	1.02
1F	1F_20_i	6.83	16.35	24.69	3.65E-04	21	3.69
1F	1F_20_j	5.52	14.99	21.61	3.82E-04	21	0.61
1F	1F_20_k	6.11	15.38	23.41	3.81E-04	21	2.41
1F	1F_20_l	5.71	14.88	22.57	3.90E-04	21	1.57
1F	1F_10_a	4.50	22.54	11.52	2.31E-04	10	1.52
1F	1F_10_b	3.94	20.84	10.90	2.49E-04	10	0.90
1F	1F_10_c	4.19	19.97	12.11	2.62E-04	10	2.11
1F	1F_10_d	3.90	19.81	11.35	2.62E-04	10	1.35
1F	1F_10_e	3.72	19.56	10.96	2.65E-04	10	0.96
1F	1F_10_f	3.85	21.37	10.38	2.42E-04	10	0.38
1F	1F_10_g	3.84	22.43	9.86	2.30E-04	10	0.14
1F	1F_10_h	3.66	19.23	10.97	2.70E-04	10	0.97
1F	1F_10_i	3.71	20.62	10.37	2.50E-04	10	0.37
1F	1F_10_j	3.51	25.70	7.85	1.98E-04	10	2.15
1F	1F_10_k	3.70	18.96	11.25	2.74E-04	10	1.25
1F	1F_10_l	3.68	19.89	10.66	2.60E-04	10	0.66

Appendix C – Raw Data (Fabric 2)

Type	Sample ID	Width (mm)	Length (mm)	Calculated Angle (deg)	Error Propagation (+/- deg)	Actual Angle (deg)	Absolute Difference (deg)
2F	2F_90_a	7.90	7.90	90.00	N/A	89	1.00
2F	2F_90_b	7.50	7.51	87.04	1.82E-02	89	1.96
2F	2F_90_c	7.92	7.95	85.02	1.02E-02	89	3.98
2F	2F_90_d	7.59	7.60	87.06	1.81E-02	89	1.94
2F	2F_90_e	7.70	7.70	90.00	N/A	89	1.00
2F	2F_90_f	7.45	7.46	87.03	1.83E-02	89	1.97
2F	2F_90_g	7.76	7.76	90.00	N/A	89	1.00
2F	2F_90_h	7.50	7.51	87.04	1.82E-02	89	1.96
2F	2F_90_i	7.05	7.07	85.69	1.33E-02	89	3.31
2F	2F_90_j	7.64	7.65	87.07	1.81E-02	89	1.93
2F	2F_90_k	7.66	7.68	85.86	1.27E-02	89	3.14
2F	2F_90_l	7.70	7.70	90.00	N/A	89	1.00
2F	2F_80_a	8.49	8.59	81.25	5.41E-03	78	3.25
2F	2F_80_b	7.74	7.89	78.81	4.62E-03	78	0.81
2F	2F_80_c	7.39	7.59	76.82	4.09E-03	78	1.18
2F	2F_80_d	7.53	7.73	76.94	4.05E-03	78	1.06
2F	2F_80_e	7.29	7.40	80.11	5.56E-03	78	2.11
2F	2F_80_f	7.87	8.07	77.22	3.96E-03	78	0.78
2F	2F_80_g	7.75	7.96	76.81	3.90E-03	78	1.19
2F	2F_80_h	7.57	7.78	76.66	3.94E-03	78	1.34
2F	2F_80_i	7.54	7.66	79.84	5.24E-03	78	1.84
2F	2F_80_j	7.62	7.74	79.90	5.17E-03	78	1.90
2F	2F_80_k	7.71	7.87	78.43	4.43E-03	78	0.43
2F	2F_80_l	7.51	7.69	77.58	4.23E-03	78	0.42
2F	2F_70_a	7.23	7.64	71.14	2.79E-03	69	2.14
2F	2F_70_b	7.26	7.71	70.33	2.65E-03	69	1.33
2F	2F_70_c	7.30	7.81	69.18	2.47E-03	69	0.18
2F	2F_70_d	7.29	7.73	70.58	2.67E-03	69	1.58
2F	2F_70_e	7.78	8.25	70.57	2.50E-03	69	1.57
2F	2F_70_f	7.23	7.81	67.78	2.31E-03	69	1.22
2F	2F_70_g	7.59	8.04	70.74	2.59E-03	69	1.74
2F	2F_70_h	7.35	7.77	71.08	2.73E-03	69	2.08
2F	2F_70_i	7.30	7.84	68.61	2.39E-03	69	0.39
2F	2F_70_j	7.11	7.67	67.97	2.37E-03	69	1.03
2F	2F_70_k	7.17	7.71	68.43	2.41E-03	69	0.57
2F	2F_70_l	7.23	7.76	68.70	2.42E-03	69	0.30

Type	Sample ID	Width (mm)	Length (mm)	Calculated Angle (deg)	Error Propagation (+/- deg)	Actual Angle (deg)	Absolute Difference (deg)
2F	2F_60_a	7.62	9.05	57.35	1.34E-03	58	0.65
2F	2F_60_b	7.56	8.64	61.04	1.59E-03	58	3.04
2F	2F_60_c	7.29	8.56	58.39	1.46E-03	58	0.39
2F	2F_60_d	7.15	8.36	58.79	1.52E-03	58	0.79
2F	2F_60_e	7.25	8.52	58.31	1.47E-03	58	0.31
2F	2F_60_f	7.20	8.37	59.34	1.55E-03	58	1.34
2F	2F_60_g	7.22	8.42	59.04	1.52E-03	58	1.04
2F	2F_60_h	7.39	8.63	58.91	1.48E-03	58	0.91
2F	2F_60_i	6.65	7.81	58.37	1.60E-03	58	0.37
2F	2F_60_j	7.03	8.32	57.67	1.47E-03	58	0.33
2F	2F_60_k	7.26	8.42	59.57	1.55E-03	58	1.57
2F	2F_60_l	6.81	7.97	58.70	1.59E-03	58	0.70
2F	2F_50_a	7.18	9.08	52.26	1.15E-03	52	0.26
2F	2F_50_b	7.11	9.09	51.46	1.12E-03	52	0.54
2F	2F_50_c	7.10	8.92	52.75	1.18E-03	52	0.75
2F	2F_50_d	6.64	8.86	48.54	1.07E-03	52	3.46
2F	2F_50_e	6.74	9.00	48.49	1.05E-03	52	3.51
2F	2F_50_f	6.15	7.89	51.21	1.28E-03	52	0.79
2F	2F_50_g	6.45	8.53	49.13	1.12E-03	52	2.87
2F	2F_50_h	6.64	8.48	51.54	1.20E-03	52	0.46
2F	2F_50_i	6.57	8.56	50.13	1.15E-03	52	1.87
2F	2F_50_j	6.18	8.06	50.06	1.22E-03	52	1.94
2F	2F_50_k	6.22	8.25	48.93	1.16E-03	52	3.07
2F	2F_50_l	6.93	8.91	51.06	1.13E-03	52	0.94
2F	2F_40_a	6.25	9.66	40.32	8.09E-04	41	0.68
2F	2F_40_b	6.13	9.60	39.68	8.03E-04	41	1.32
2F	2F_40_c	6.19	9.81	39.12	7.77E-04	41	1.88
2F	2F_40_d	6.28	9.30	42.48	8.80E-04	41	1.48
2F	2F_40_e	6.69	10.41	39.99	7.45E-04	41	1.01
2F	2F_40_f	6.03	9.05	41.78	8.90E-04	41	0.78
2F	2F_40_g	6.29	9.28	42.67	8.85E-04	41	1.67
2F	2F_40_h	6.09	9.31	40.85	8.48E-04	41	0.15
2F	2F_40_i	6.56	9.97	41.15	7.97E-04	41	0.15
2F	2F_40_j	6.42	9.81	40.88	8.06E-04	41	0.12
2F	2F_40_k	5.77	8.75	41.26	9.11E-04	41	0.26
2F	2F_40_l	6.44	9.91	40.53	7.92E-04	41	0.47

Type	Sample ID	Width (mm)	Length (mm)	Calculated Angle (deg)	Error Propagation (+/- deg)	Actual Angle (deg)	Absolute Difference (deg)
2F	2F_30_a	5.99	10.79	33.72	6.37E-04	31	2.72
2F	2F_30_b	5.86	11.53	30.55	5.65E-04	31	0.45
2F	2F_30_c	5.35	10.24	31.50	6.46E-04	31	0.50
2F	2F_30_d	5.86	11.30	31.24	5.83E-04	31	0.24
2F	2F_30_e	5.83	10.74	32.88	6.31E-04	31	1.88
2F	2F_30_f	5.86	10.59	33.60	6.48E-04	31	2.60
2F	2F_30_g	5.41	10.56	30.82	6.19E-04	31	0.18
2F	2F_30_h	5.87	10.95	32.42	6.14E-04	31	1.42
2F	2F_30_i	5.54	10.40	32.19	6.44E-04	31	1.19
2F	2F_30_j	5.51	10.43	31.89	6.39E-04	31	0.89
2F	2F_30_k	5.57	11.00	30.42	5.91E-04	31	0.58
2F	2F_30_l	5.63	11.16	30.30	5.81E-04	31	0.70
2F	2F_20_a	4.70	12.44	22.20	4.64E-04	21	1.20
2F	2F_20_b	5.09	14.14	21.10	4.03E-04	21	0.10
2F	2F_20_c	5.06	14.00	21.19	4.07E-04	21	0.19
2F	2F_20_d	4.91	13.88	20.72	4.09E-04	21	0.28
2F	2F_20_e	5.26	14.22	21.71	4.04E-04	21	0.71
2F	2F_20_f	4.89	13.36	21.47	4.28E-04	21	0.47
2F	2F_20_g	5.15	14.31	21.09	3.98E-04	21	0.09
2F	2F_20_h	4.96	12.52	23.34	4.68E-04	21	2.34
2F	2F_20_i	5.24	12.96	23.85	4.55E-04	21	2.85
2F	2F_20_j	4.82	13.86	20.35	4.07E-04	21	0.65
2F	2F_20_k	4.91	13.21	21.82	4.35E-04	21	0.82
2F	2F_20_l	5.21	15.07	20.23	3.74E-04	21	0.77
2F	2F_10_a	3.77	21.81	9.95	2.36E-04	10	0.05
2F	2F_10_b	4.25	20.79	11.80	2.51E-04	10	1.80
2F	2F_10_c	4.08	21.25	11.07	2.44E-04	10	1.07
2F	2F_10_d	3.73	20.77	10.35	2.49E-04	10	0.35
2F	2F_10_e	4.29	20.88	11.86	2.50E-04	10	1.86
2F	2F_10_f	4.01	20.82	11.10	2.49E-04	10	1.10
2F	2F_10_g	3.87	18.74	11.92	2.78E-04	10	1.92
2F	2F_10_h	3.60	19.70	10.53	2.62E-04	10	0.53
2F	2F_10_i	3.78	20.44	10.66	2.53E-04	10	0.66
2F	2F_10_j	3.68	20.49	10.35	2.52E-04	10	0.35
2F	2F_10_k	3.84	21.98	10.06	2.35E-04	10	0.06
2F	2F_10_l	3.70	19.75	10.80	2.62E-04	10	0.80

Appendix D – Bloodstain Images (Control)

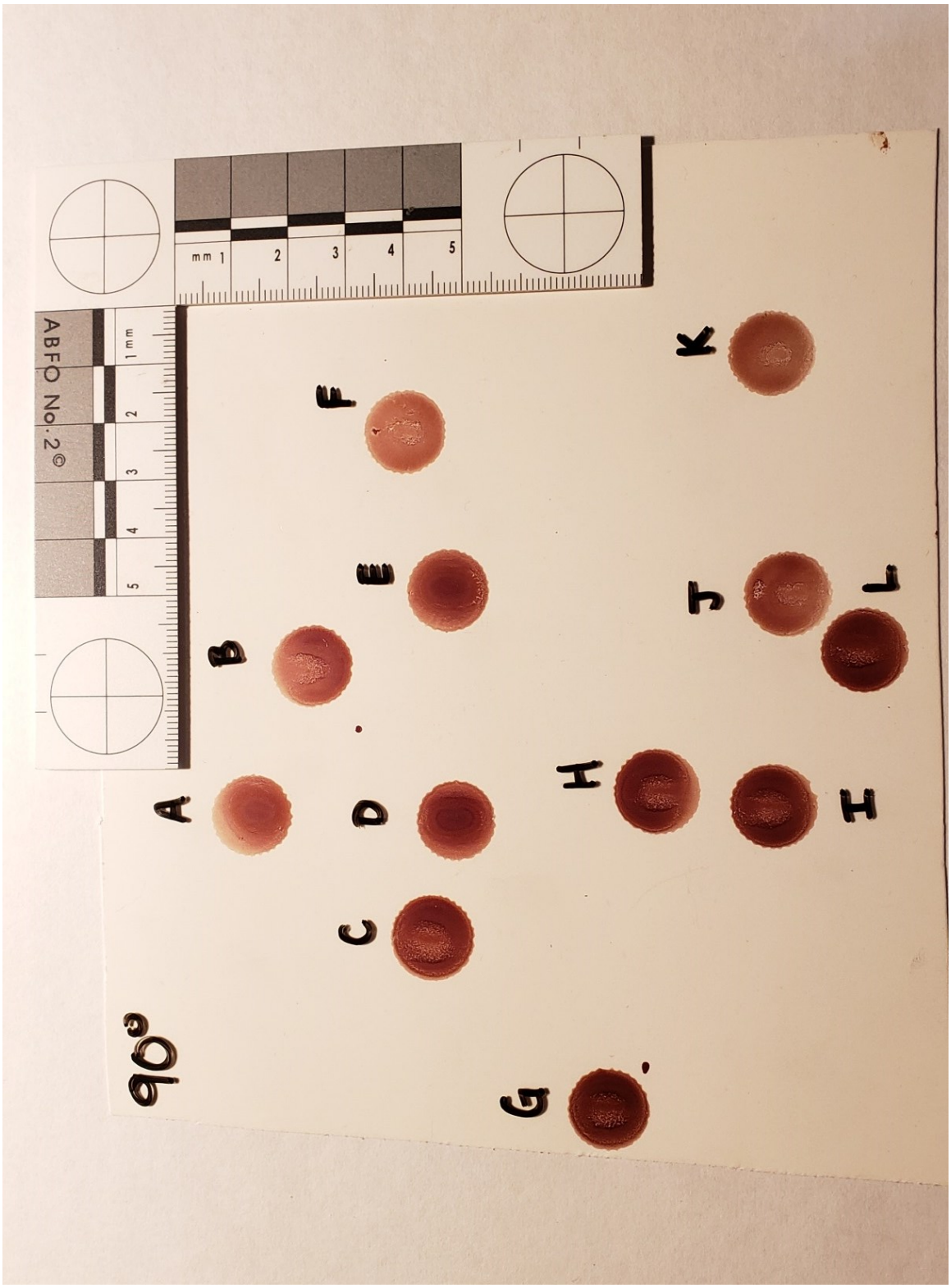

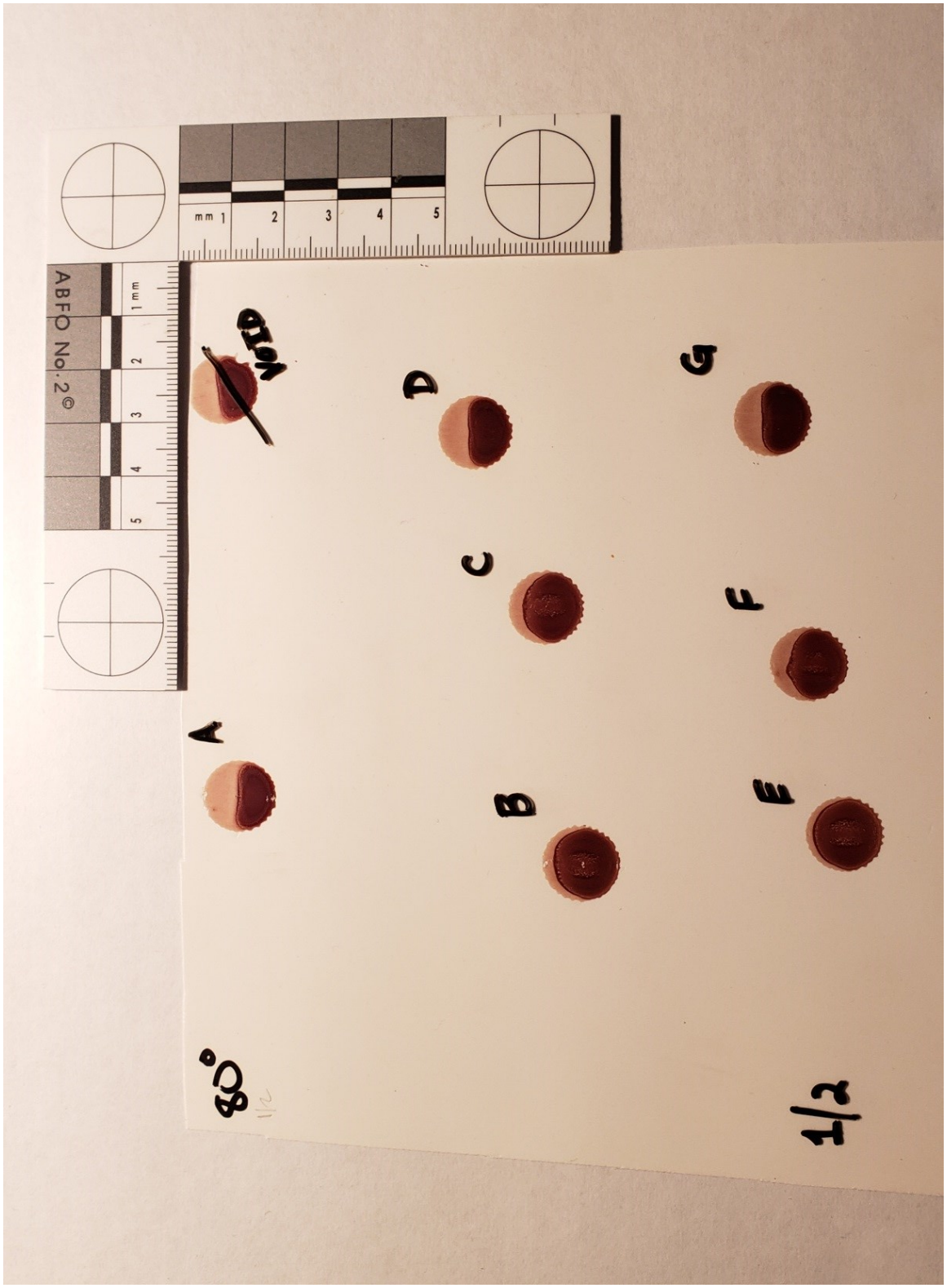
ABFO No.2©
mm 1 2 3 4 5
VOID
A
B
C
D
E
F
G
80°
1/2

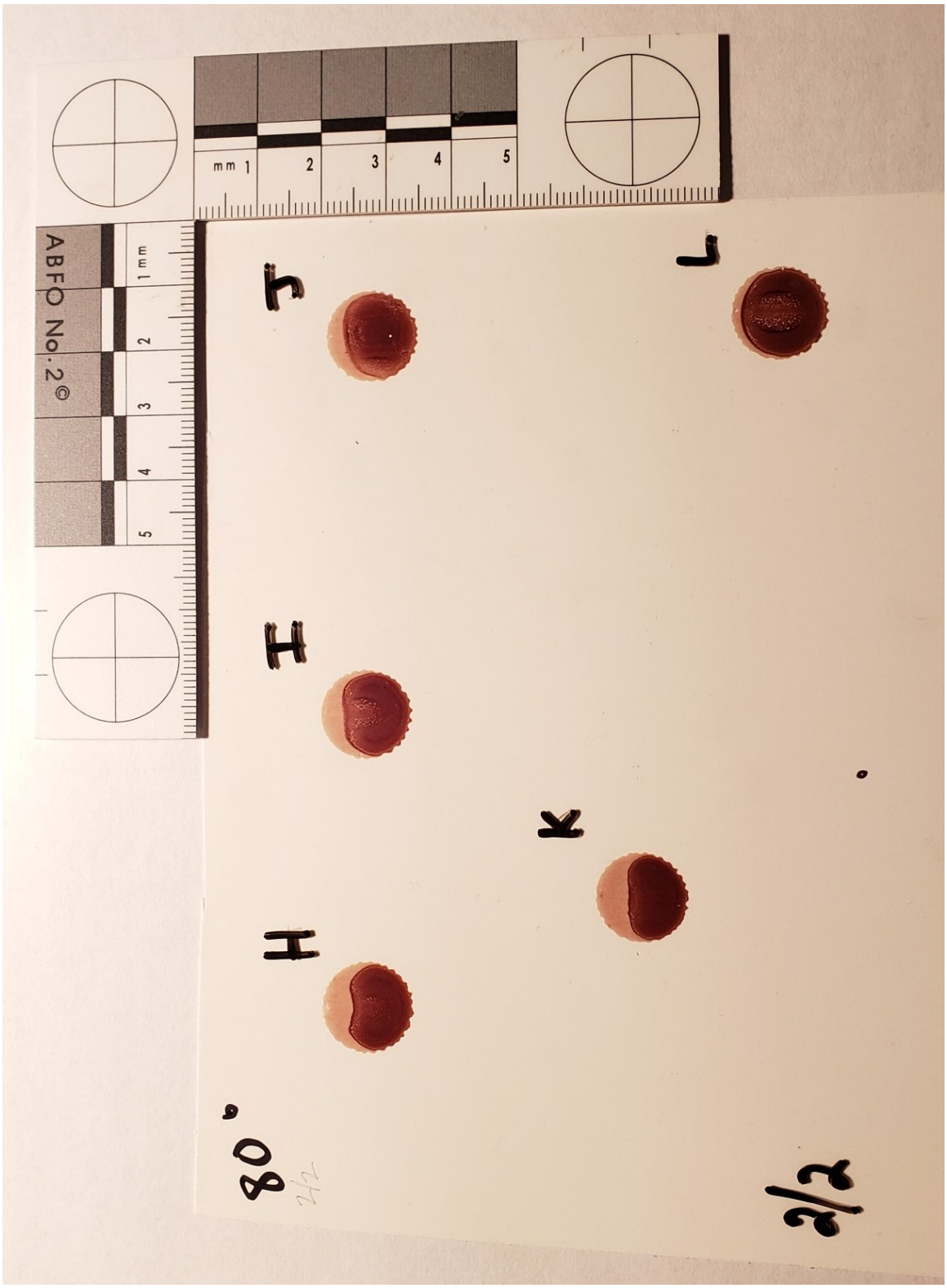
ABFO No. 2©
mm 1 2 3 4 5
80°
2/2

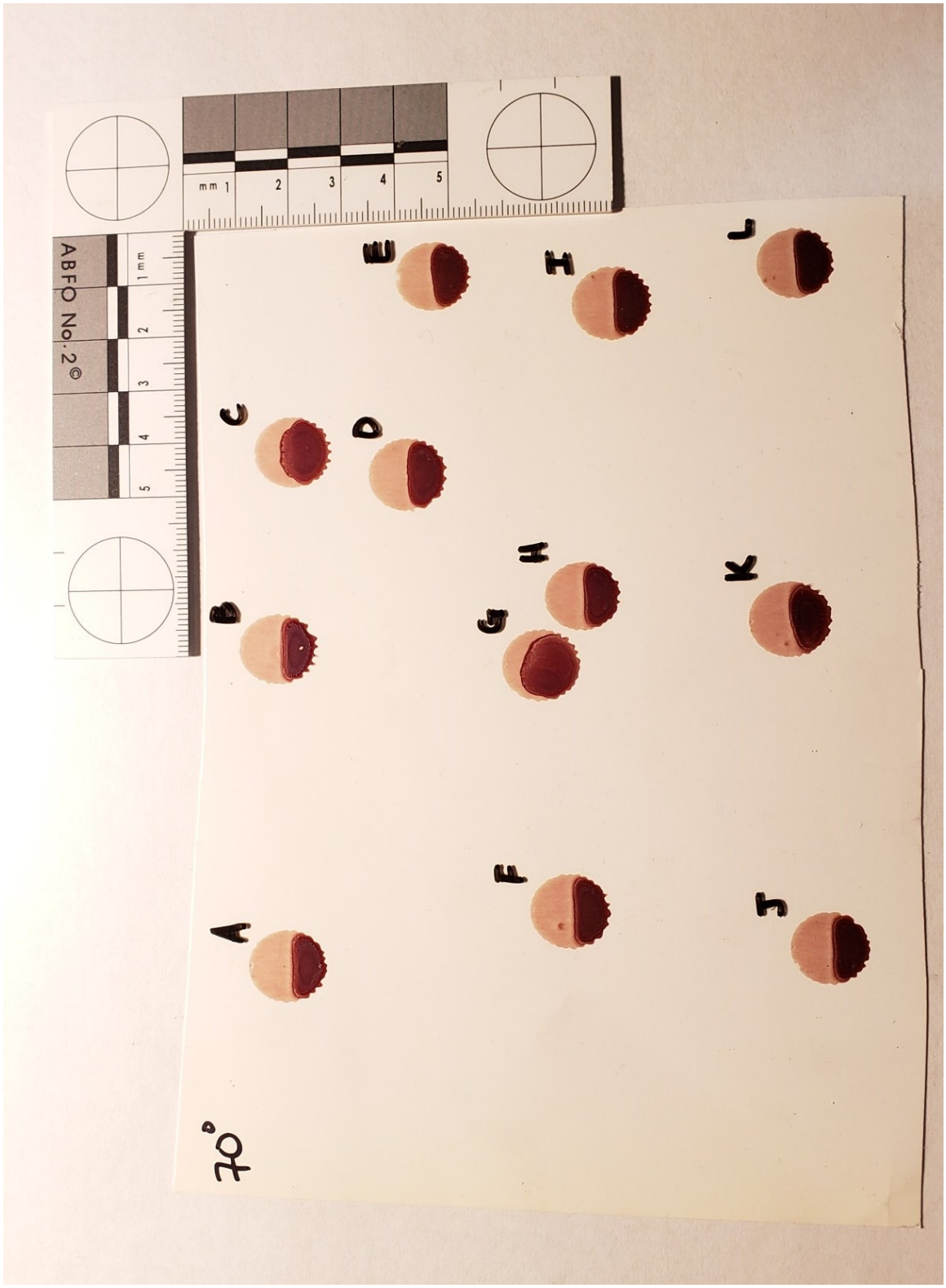
ABFO No. 2©
mm 1 2 3 4 5
A
B
C
D
E
F
G
H
H
J
K
L
70°

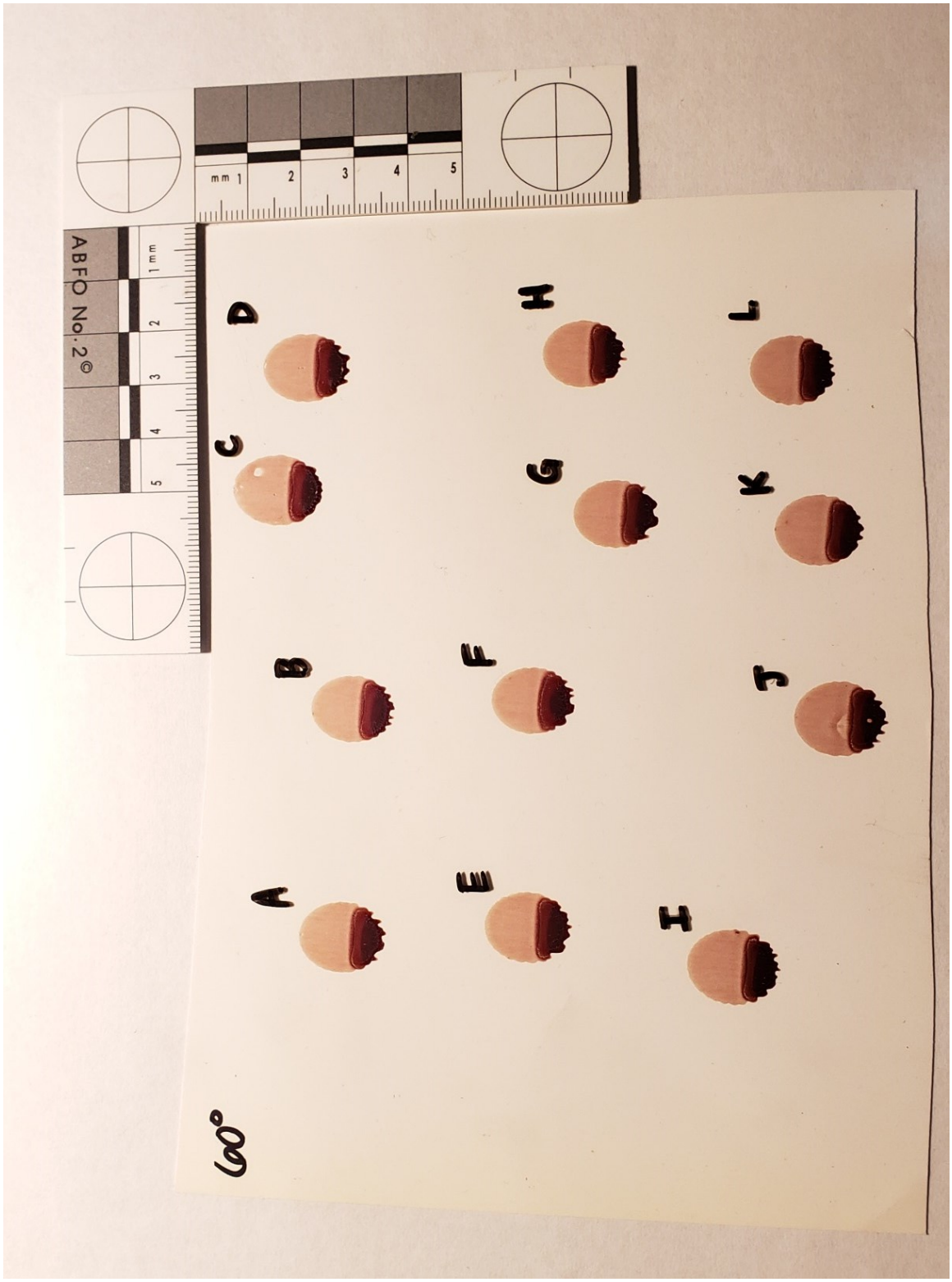
ABFO No. 2©
mm 1 2 3 4 5
1 mm 2 3 4 5
D
H
L
C
G
K
B
F
J
A
E
I
90°

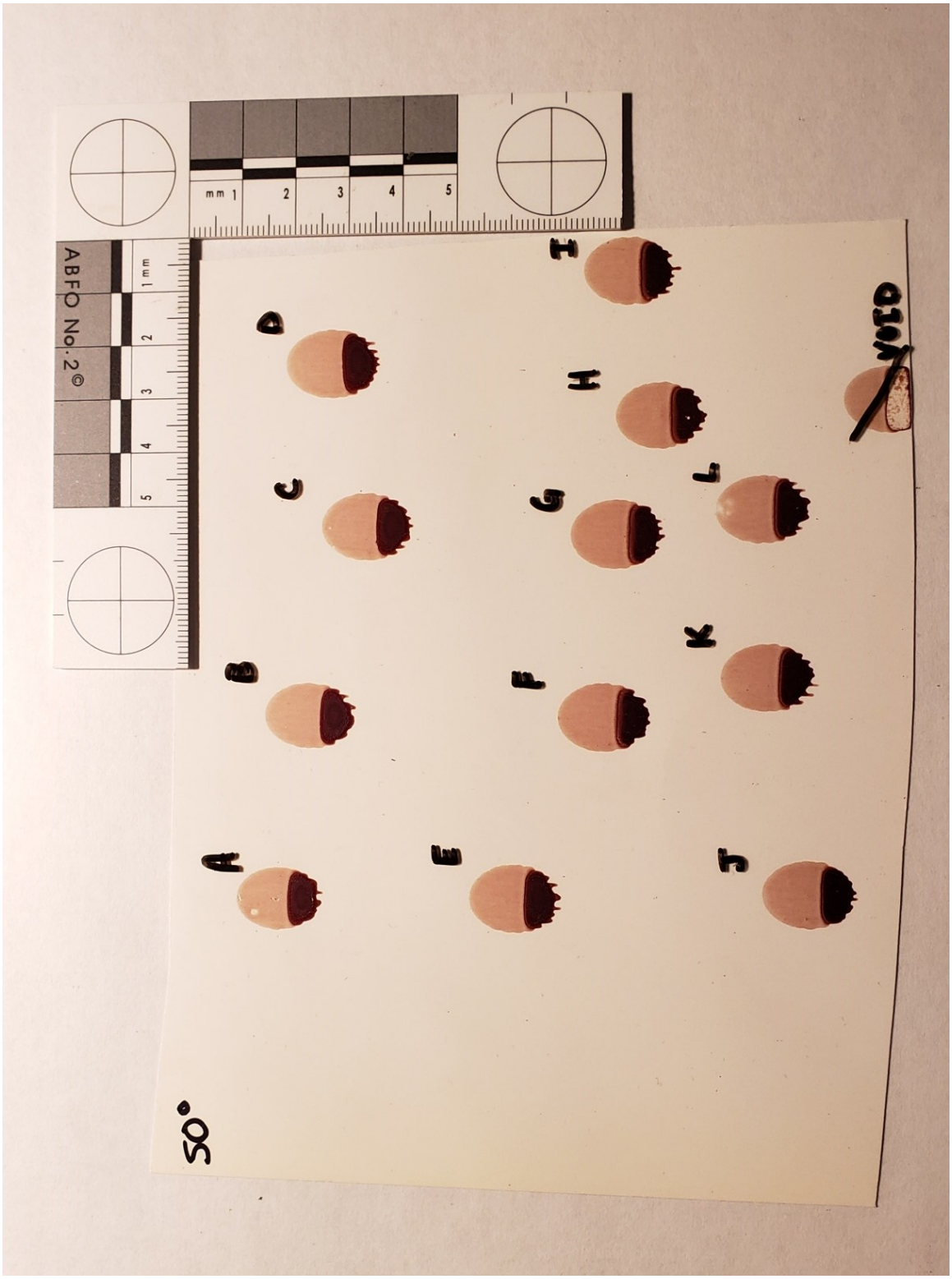
ABFO No. 2©
mm 1 2 3 4 5
1 mm 2 3 4 5
A
B
C
D
E
F
G
H
I
J
K
L
WOOD
30°

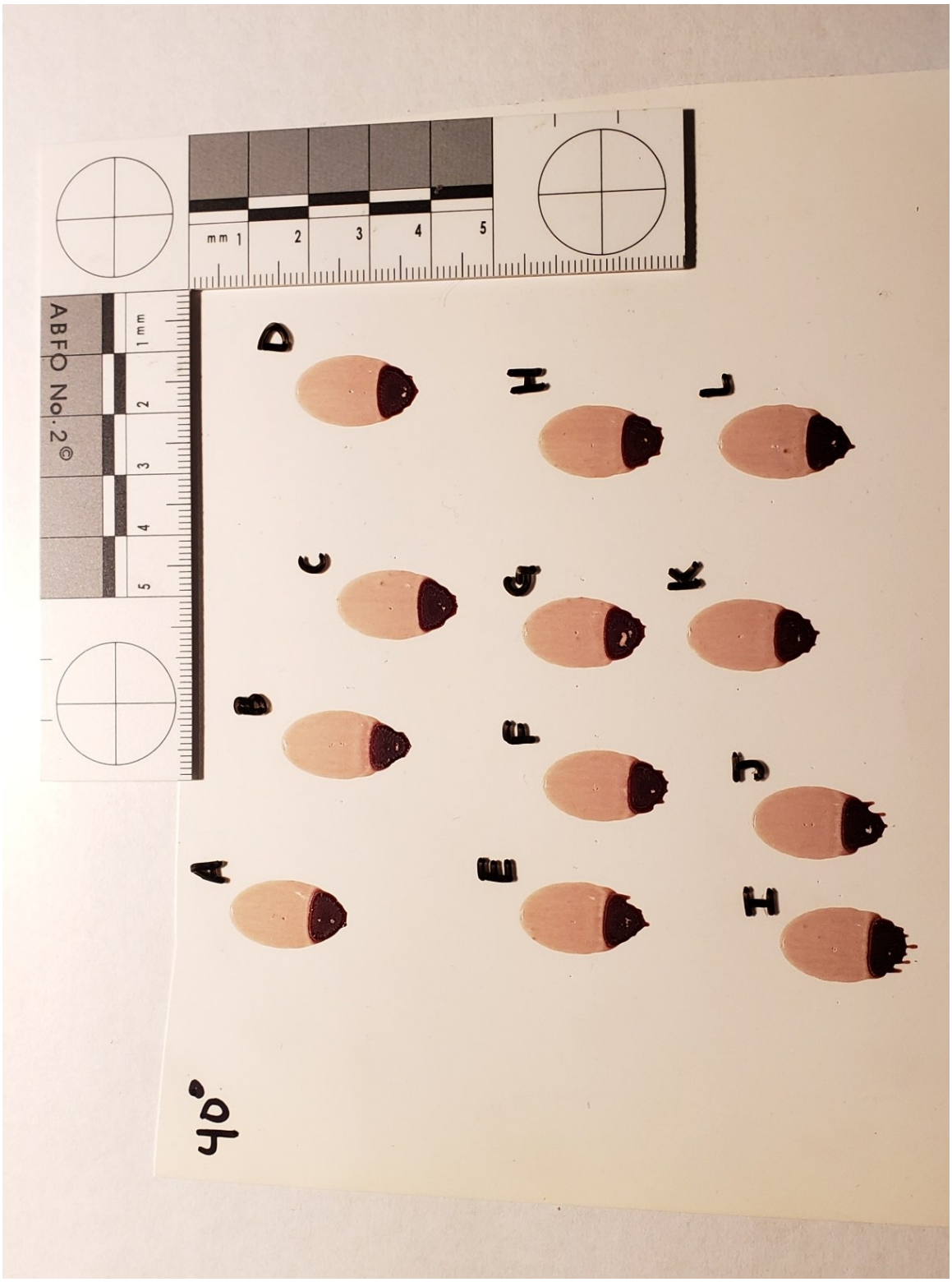
ABFO No. 2©
mm 1
2
3
4
5
A
B
C
D
E
F
G
H
I
J
K
L
90°

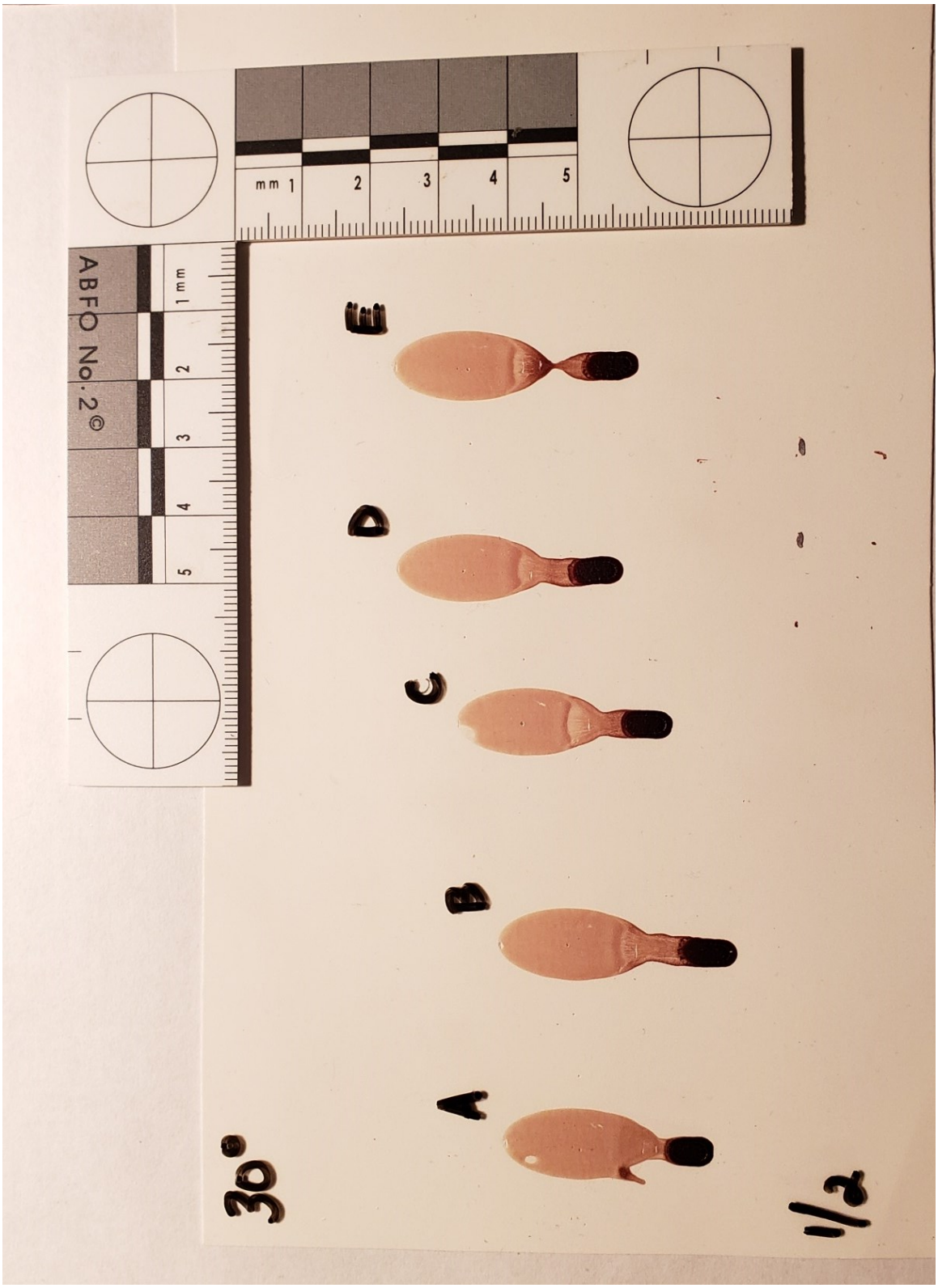
ABFO No. 2©
mm 1 2 3 4 5
E
D
C
B
A
30°
1/2

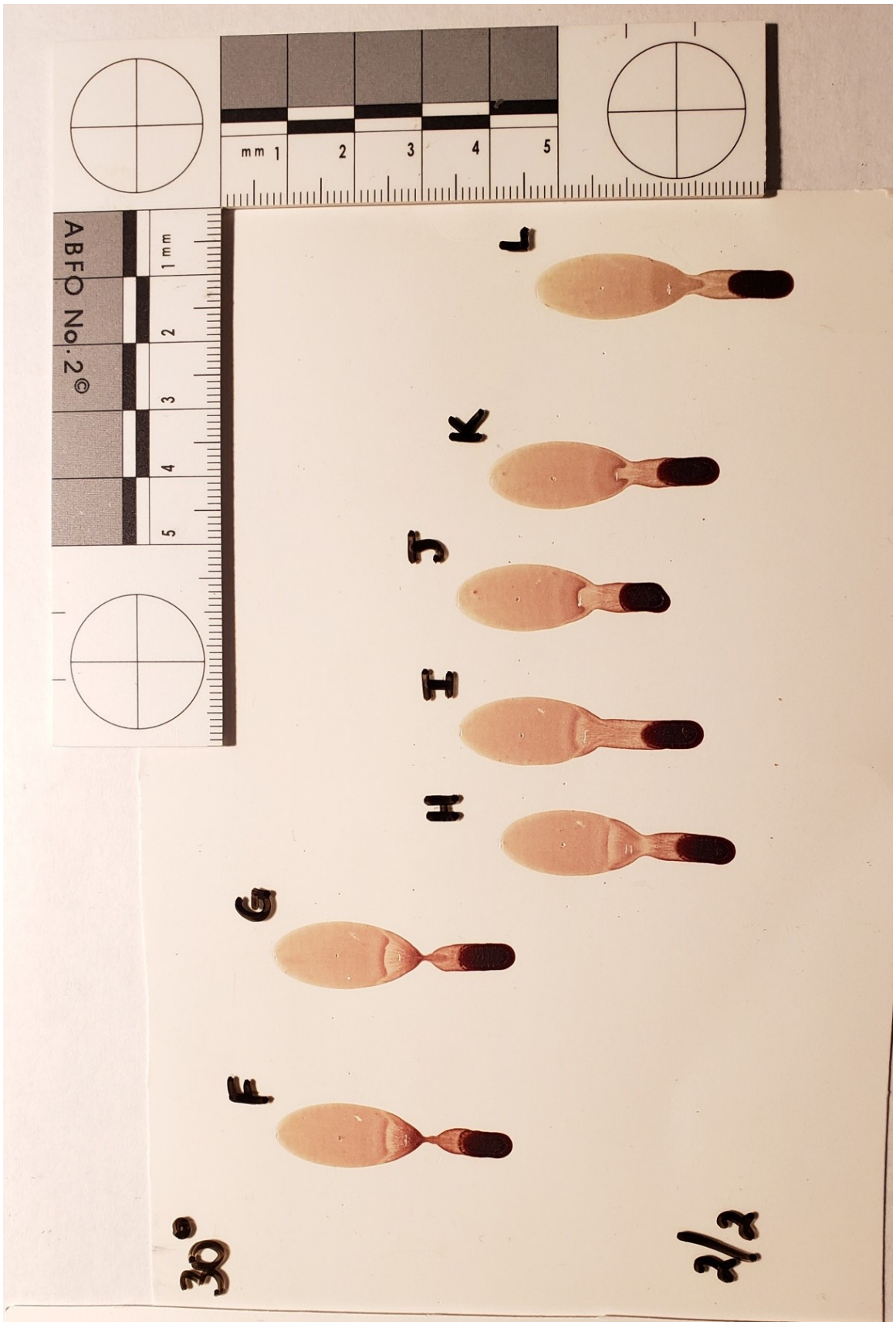
ABFO No. 2©
mm 1 2 3 4 5
1 mm 2 3 4 5
J
K
I
H
H
G
F
30°
2/2

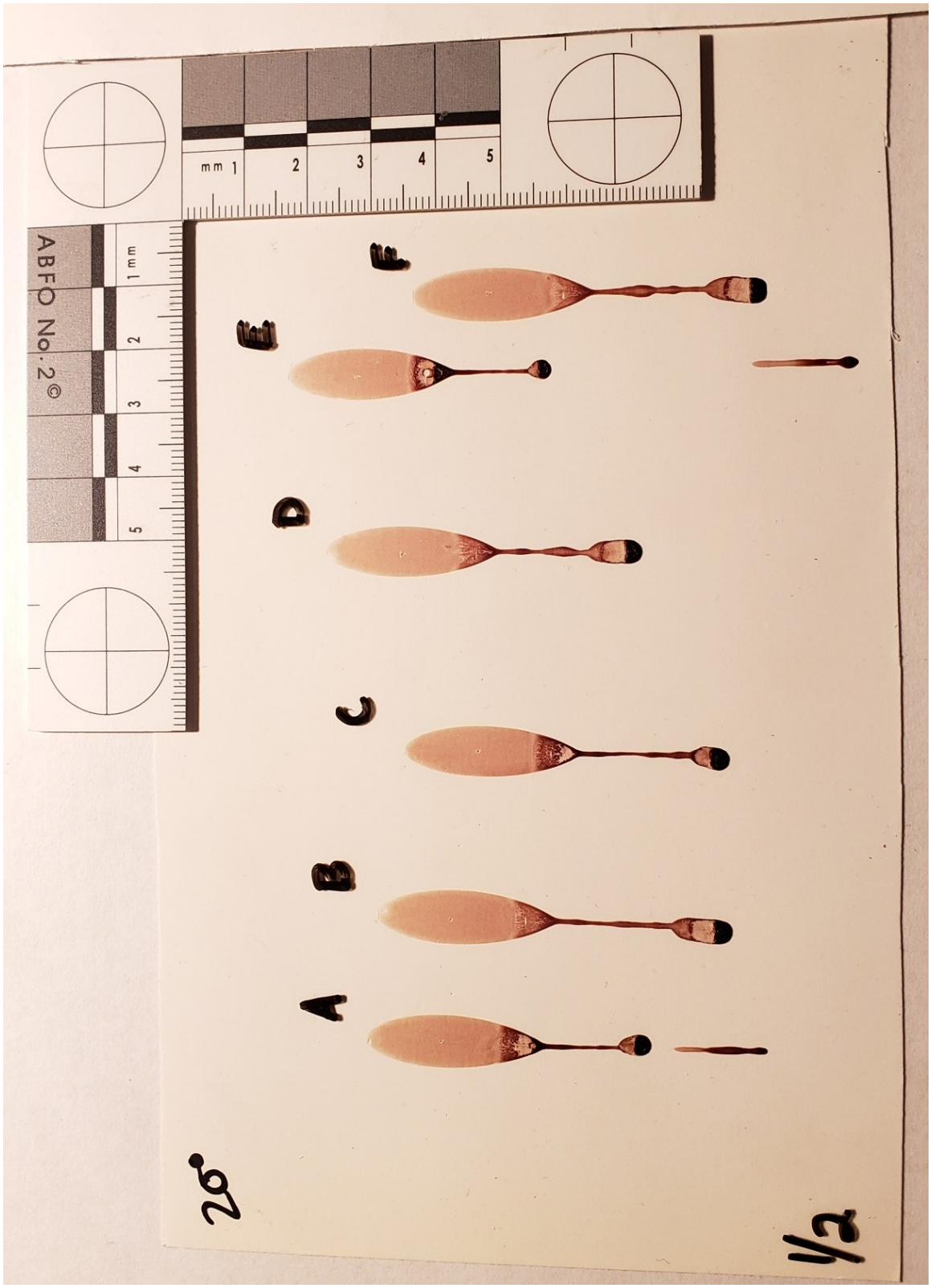
ABFO No. 2©
mm 1
2
3
4
5
A
B
C
D
E
E
20°
1/2

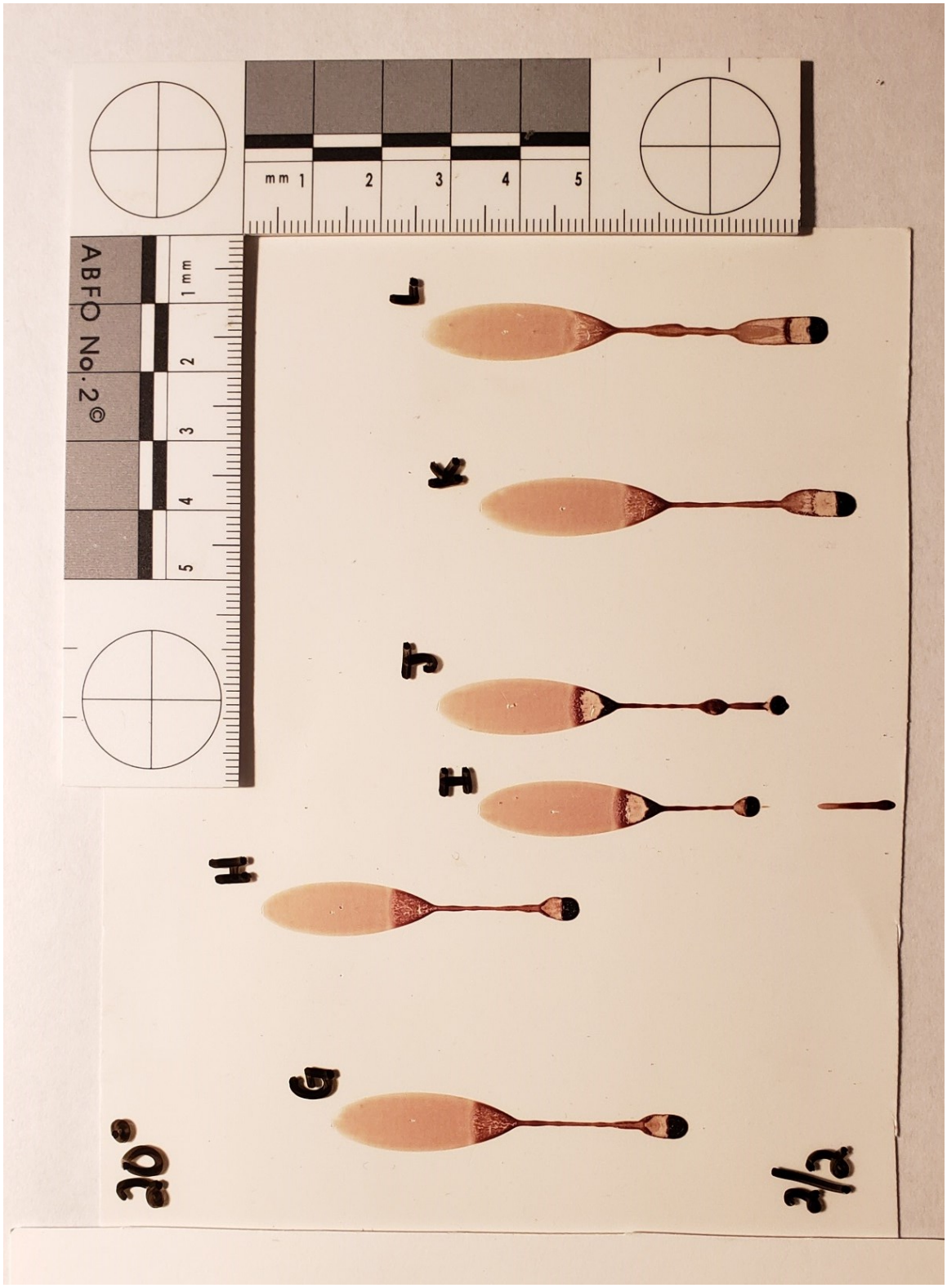
ABFO No.2©
mm 1 2 3 4 5
1 mm 2 3 4 5
J
K
I
H
H
G
30°
45°

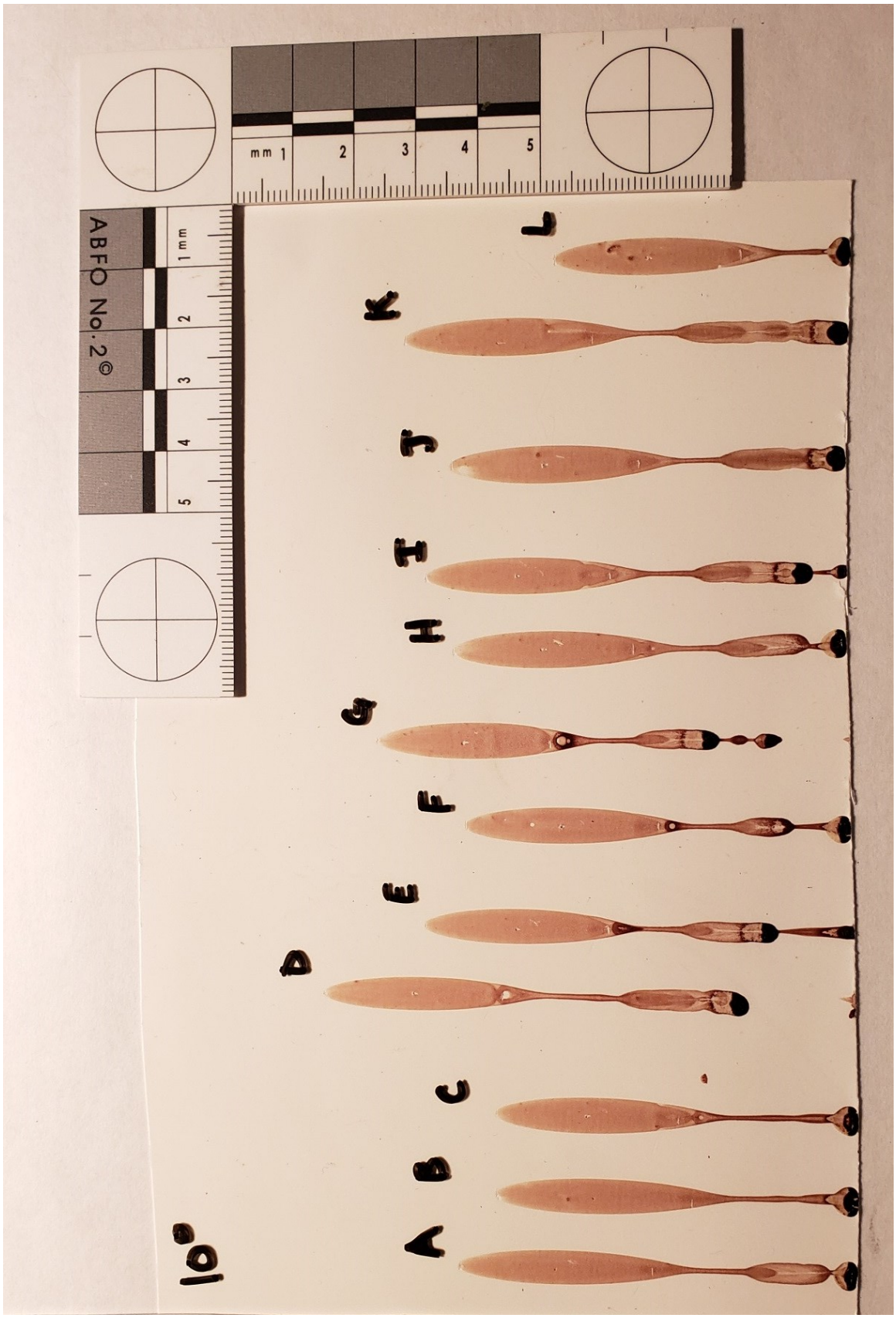
ABFO No. 2©
mm 1 2 3 4 5
10°
A B C D E F G H I J K L

Appendix E – Bloodstain Images (Fabric 1)

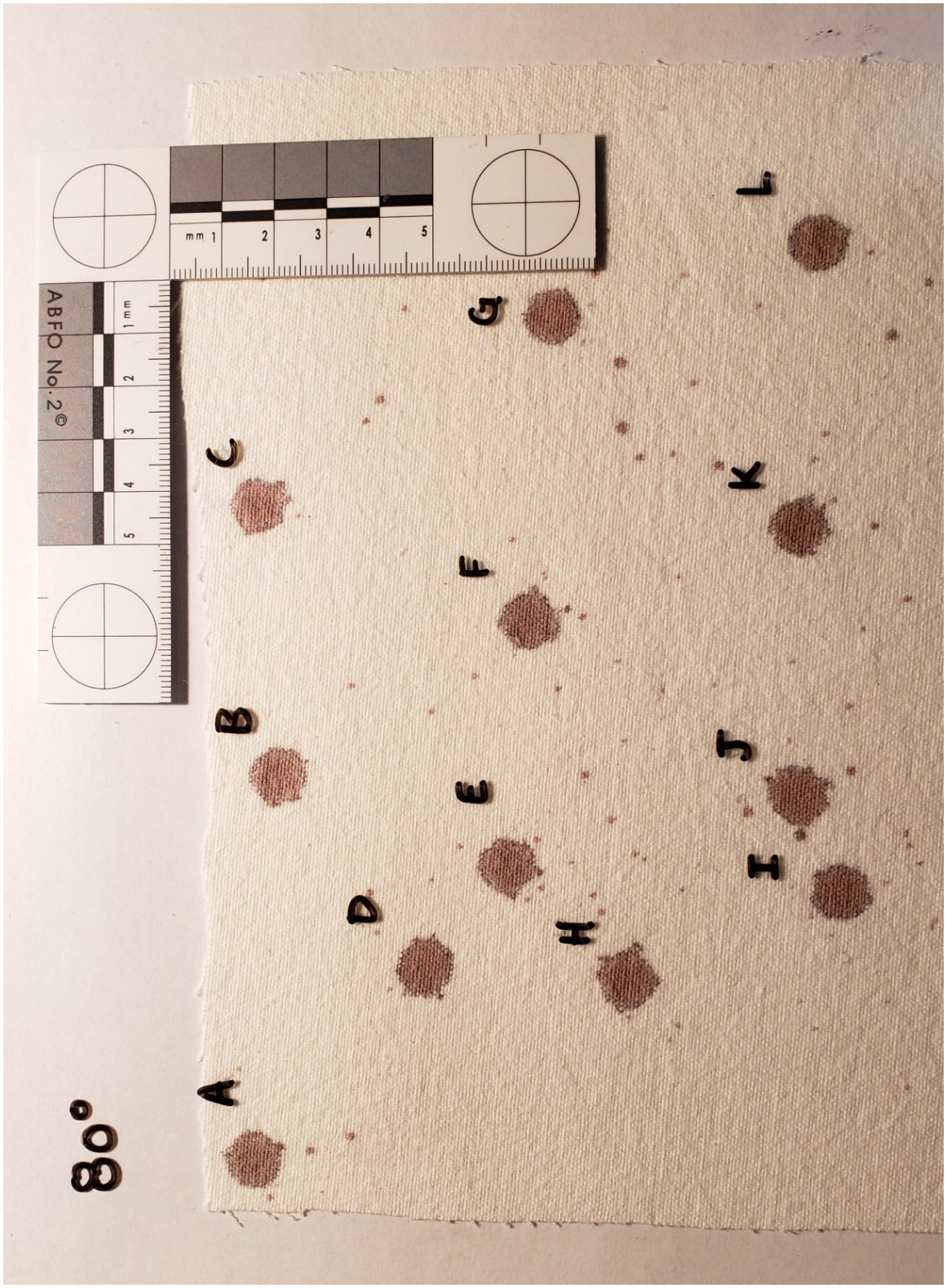
ABFO No. 2©
mm 1 2 3 4 5
80°
A
B
C
D
E
F
G
H
I
J
K
L


ABFO No. 2©
mm 1 2 3 4 5
1 mm 2 3 4 5
E
I
D
H
J
H
C
B
G
K
A
F


ABFO No.2©
mm 1 2 3 4 5
A
B
C
D
E
F
G
H
I
J
K
L
VOID
60°


ABFO No. 2©
mm 1 2 3 4 5
A
B
C
D
E
F
G
H
I
J
K
L
50.

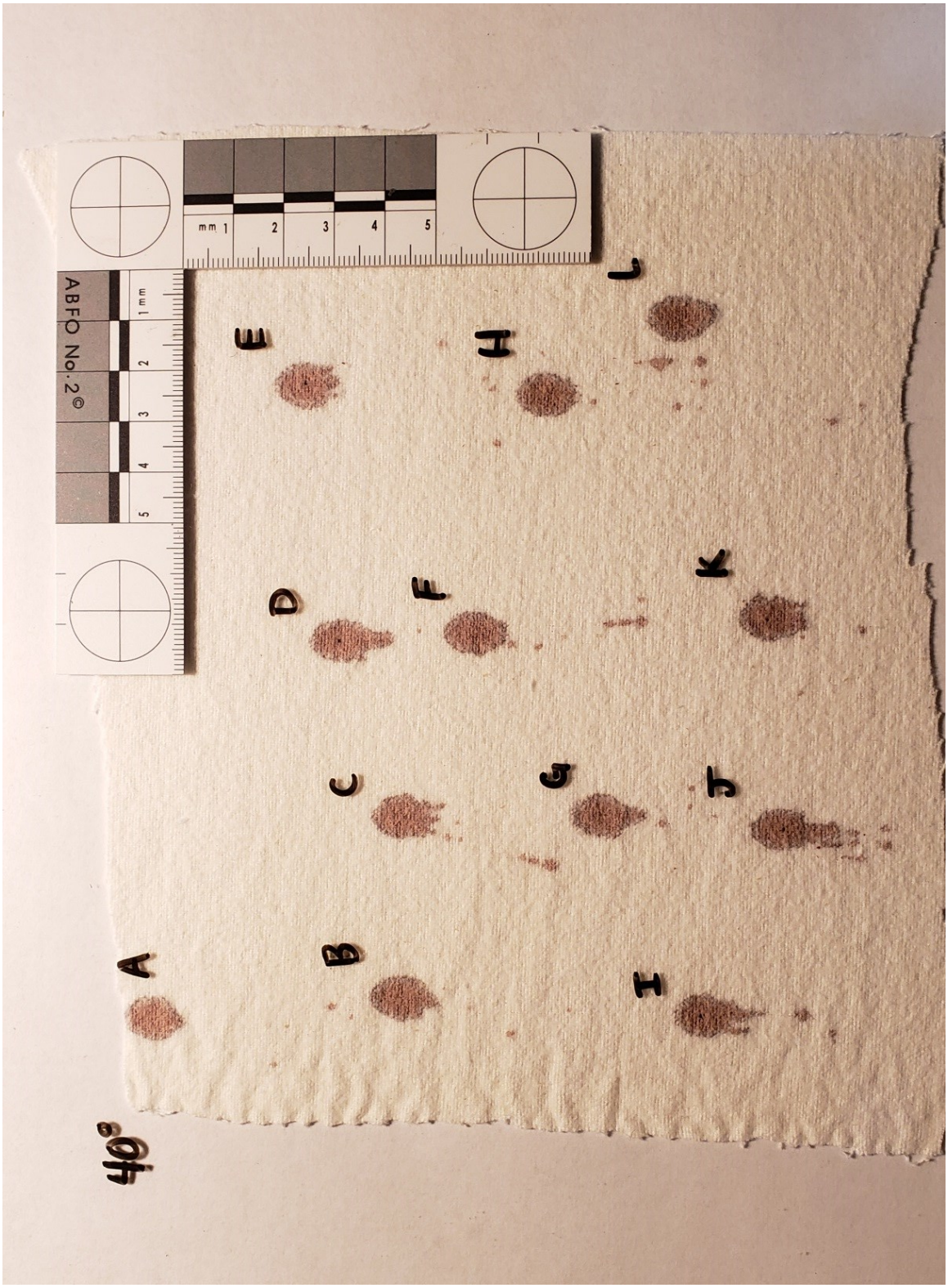
mm 1 2 3 4 5
ABFO No. 2 ©
1 mm 2 3 4 5
A
B
C
D
E
F
G
H
I
J
K
90°

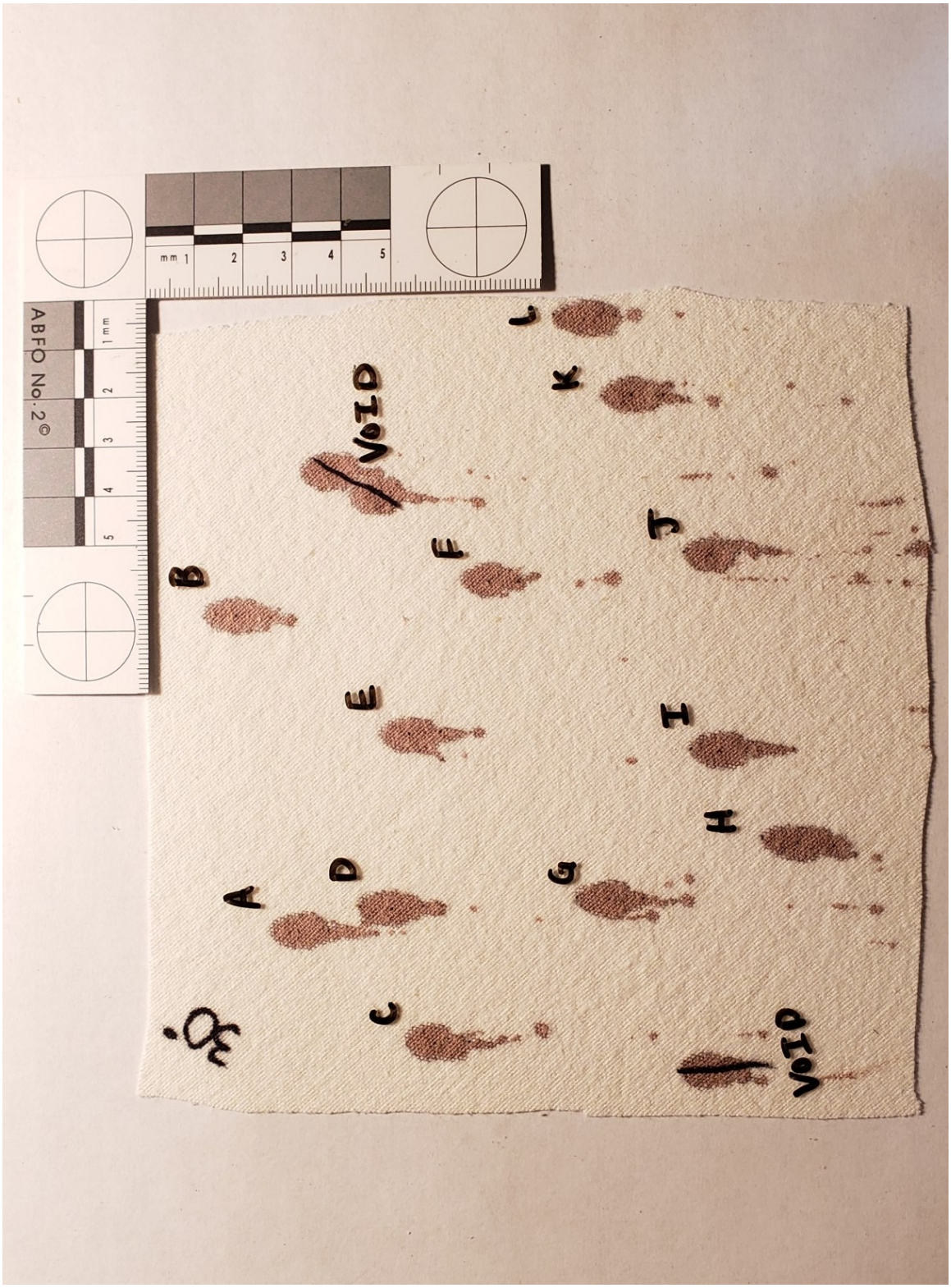
ABFO No.2©
mm 1 2 3 4 5
A
B
C
D
E
F
G
H
I
J
K
L
VOID
VOID

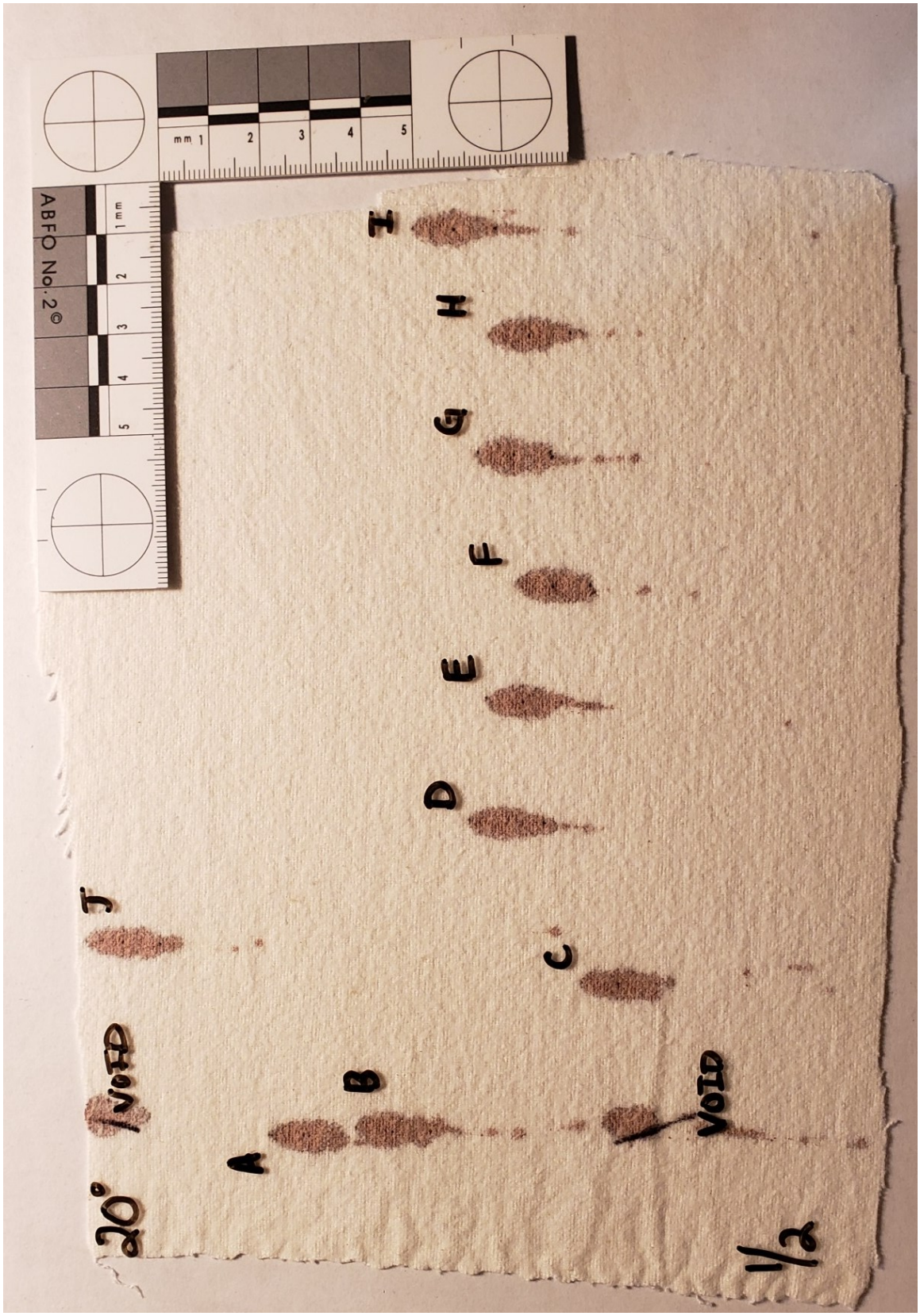
ABFO No. 2©
mm 1 2 3 4 5
1 mm 2 3 4 5
I
H
G
F
E
D
C
J
B
A
VOID
VOID
20°
1/2


mm 1
2
3
4
5
ABFO No. 2©
1 mm
2
3
4
5
L
K
20.
2/2


ABFO No. 2©
mm 1 2 3 4 5
E
D
VOID
C
B
A
.01
1/2


ABFO No.2©
mm 1 2 3 4 5
L
K
J
I
H
G
F
E
2/2

Appendix F – Bloodstain Images (Fabric 2)

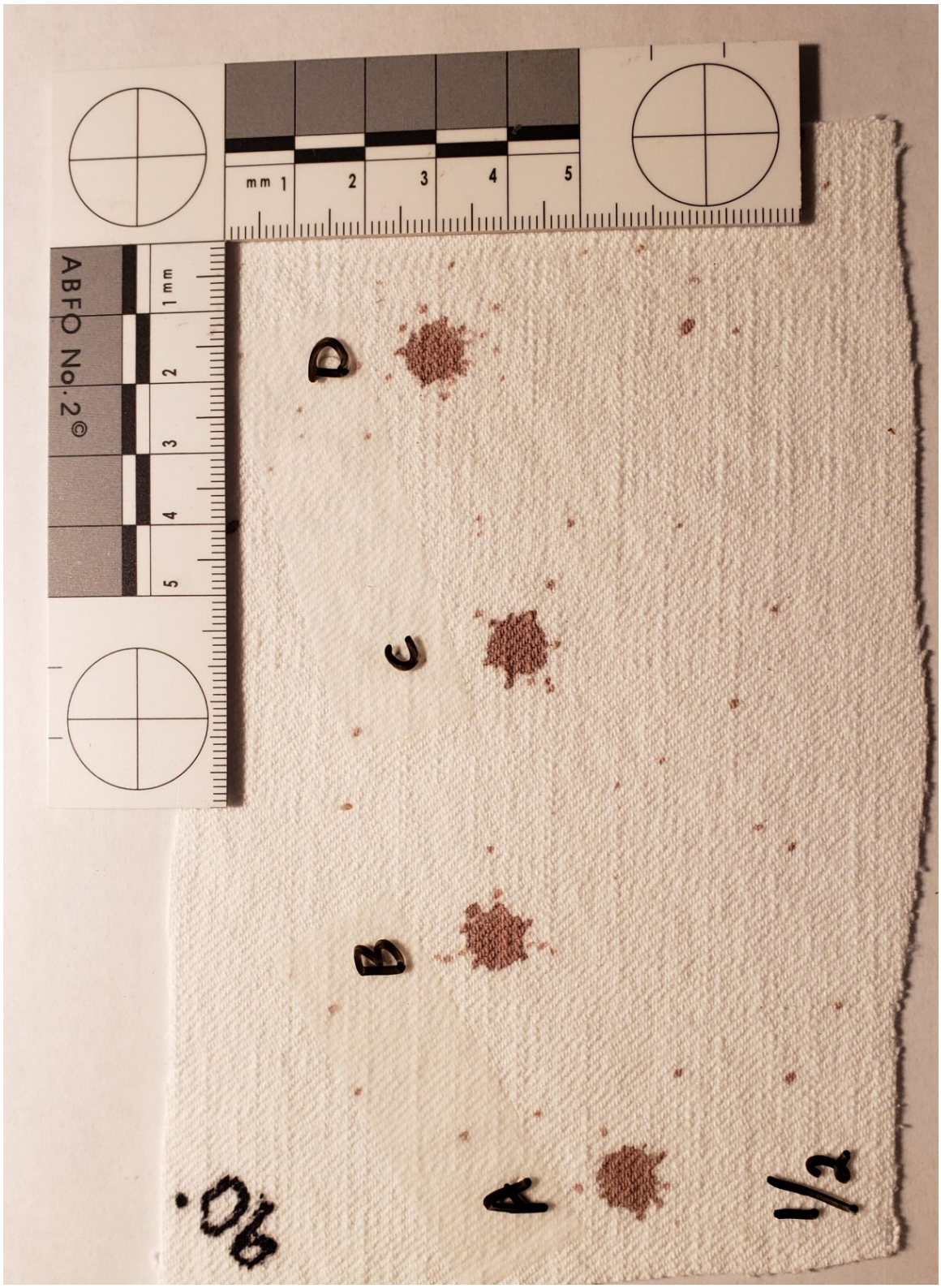

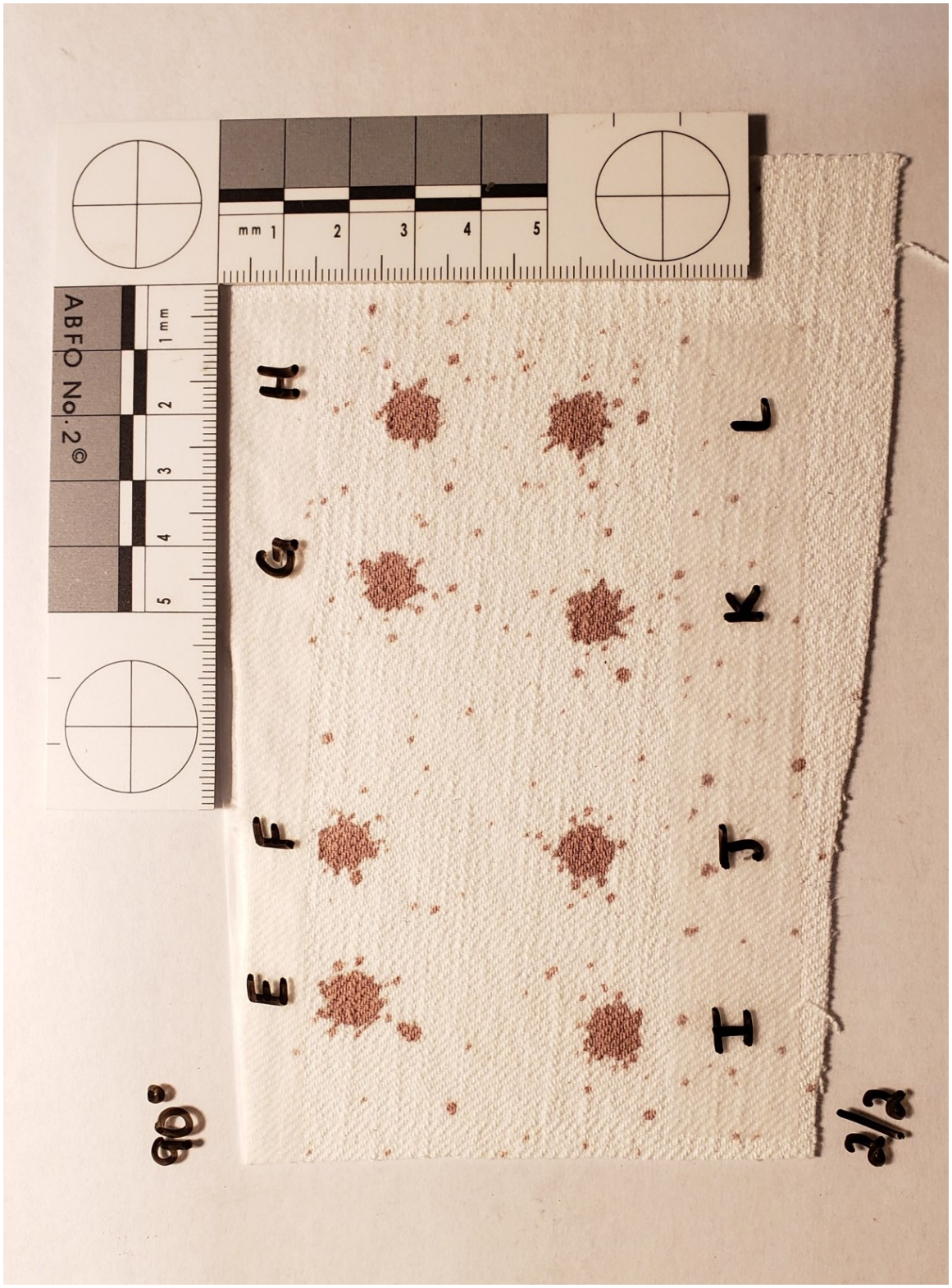
ABFO No. 2©
mm 1 2 3 4 5
1 mm 2 3 4 5
H
G
F
E
L
K
J
I
90°
2/2

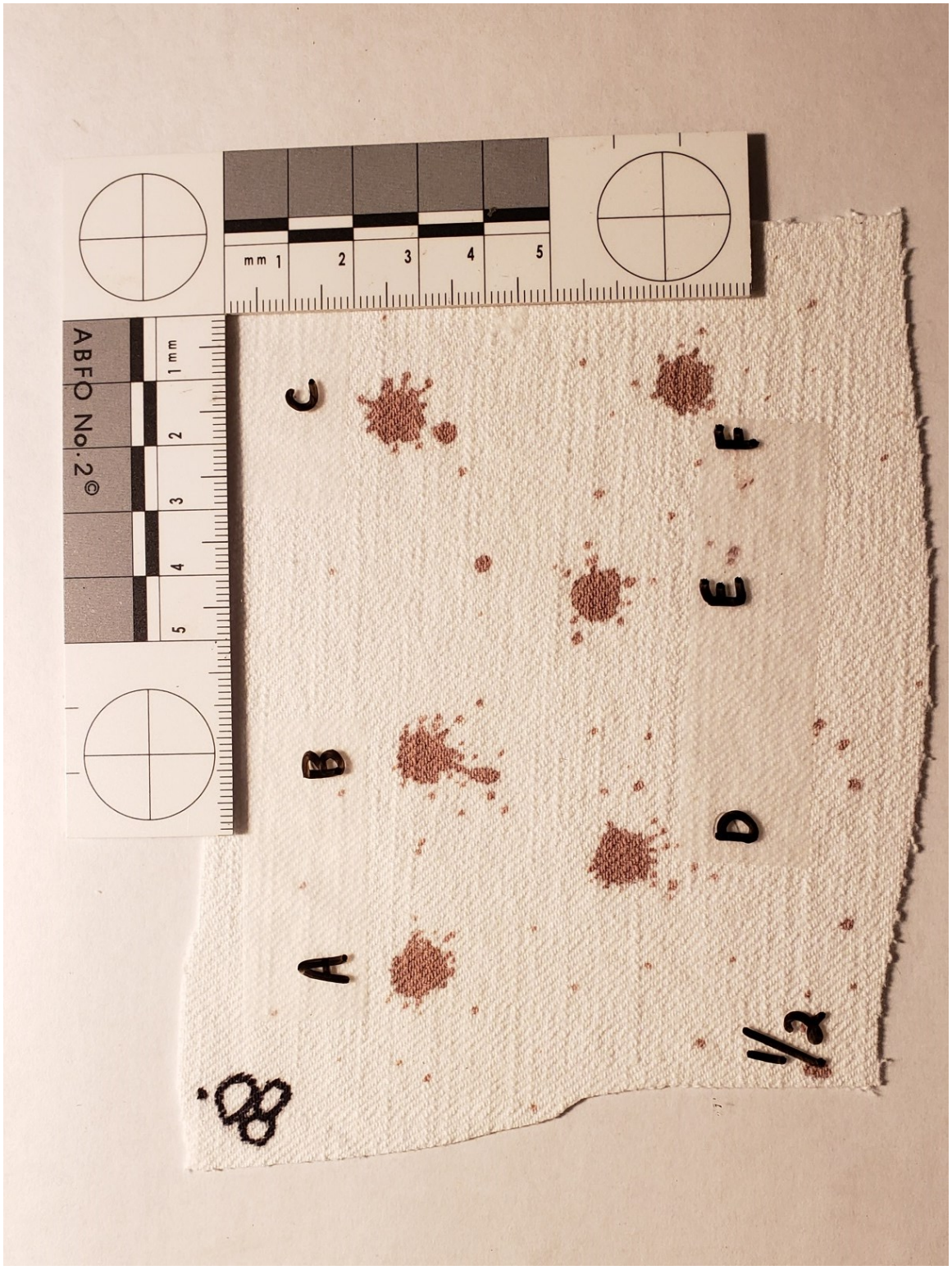
ABFO No. 2©
mm 1 2 3 4 5
A
B
C
D
E
F
.08
1/2


ABFO No.2©
mm 1 2 3 4 5
H
L
VOID
H
K
J
G
VOID
21/2

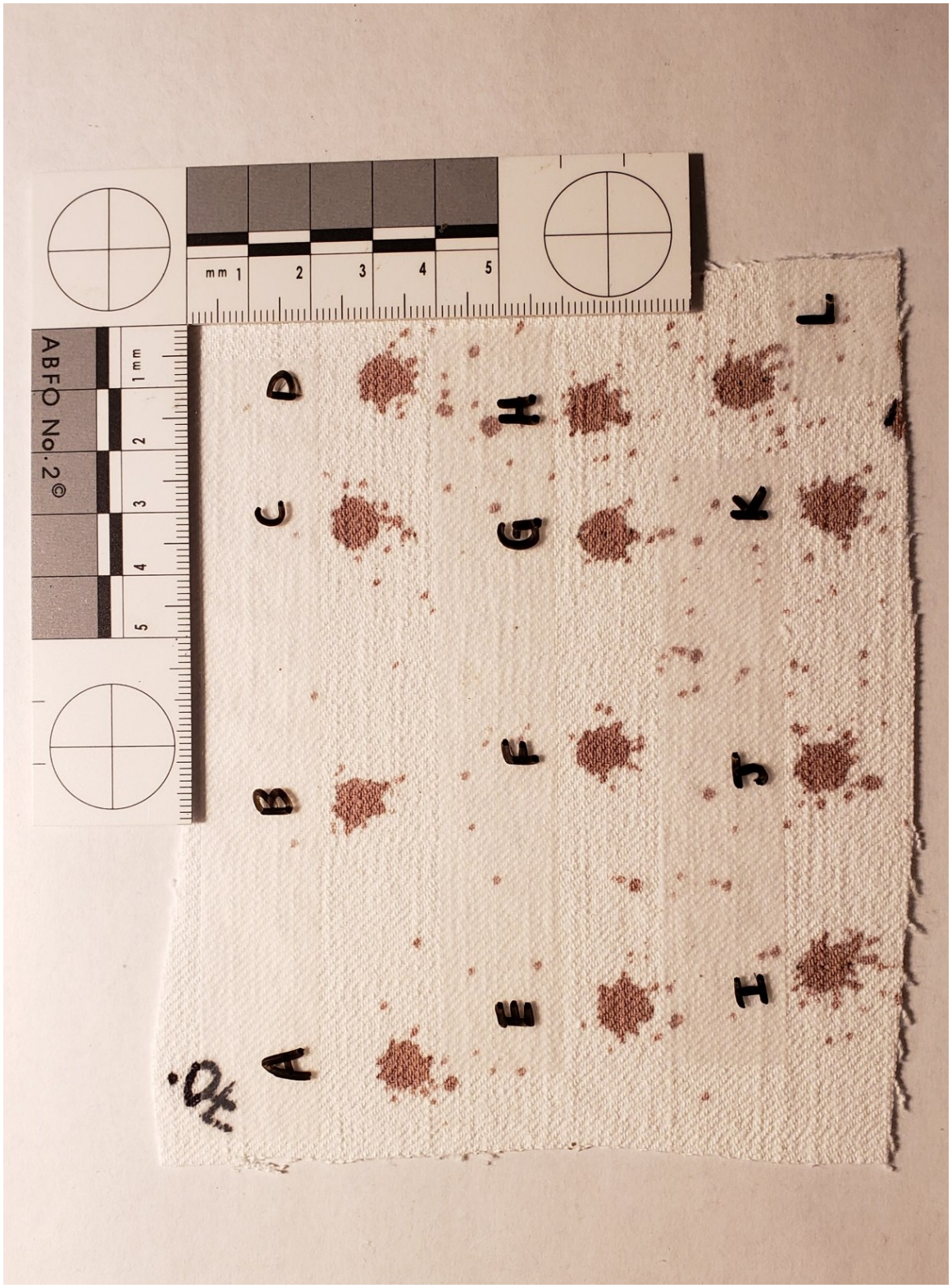
ABFO No.2©
mm 1
2
3
4
5
A
B
C
D
E
F
G
H
I
J
K
L


ABFO No. 2©
mm 1 2 3 4 5
A
B
C
D
E
F
G
H
I
H
L
K
60°


ABFO No.2©
mm 1 2 3 4 5
1 mm 2 3 4 5
F L
E K
D J
C H
B H
A G
50.05


ABFO No. 2©
mm 1 2 3 4 5
A
B
C
D
E
F
90°
Void
1/2

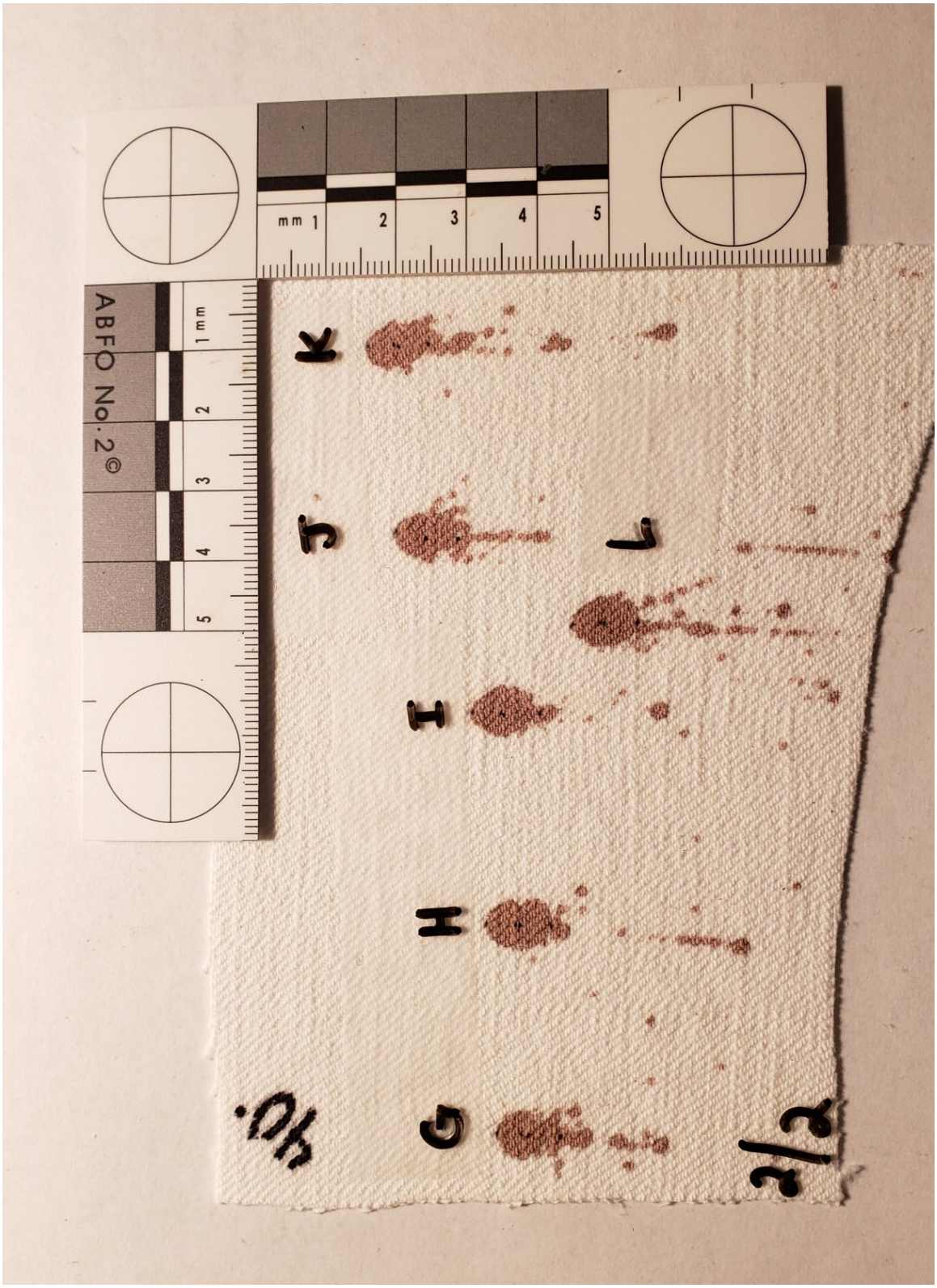
mm 1
2
3
4
5
ABFO No. 2©
1 mm
2
3
4
5
K
J
I
H
G
#0.
2/2

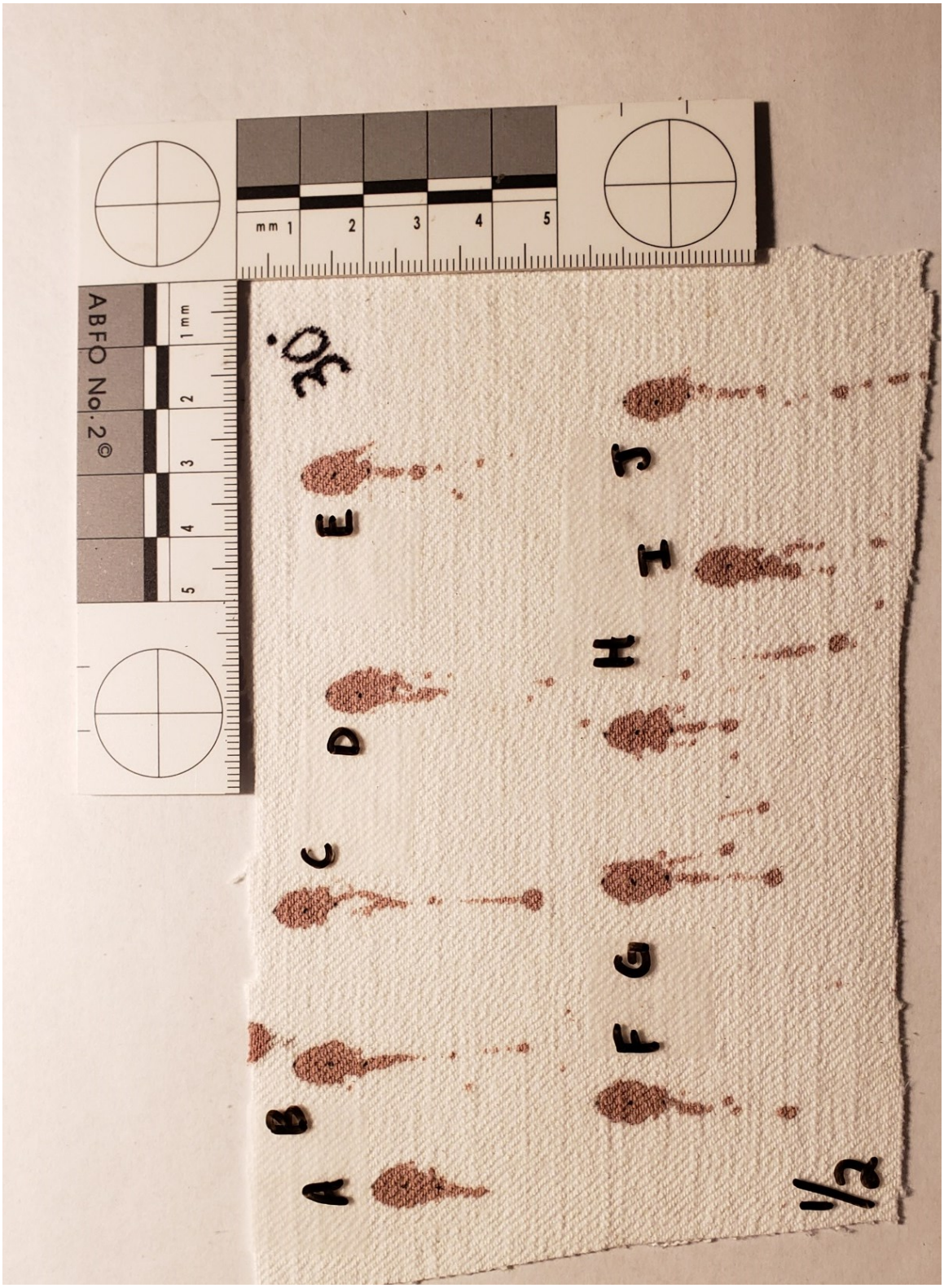
ABFO No. 2©
mm 1 2 3 4 5
30°
A
B
C
D
E
F
G
H
I
1/2

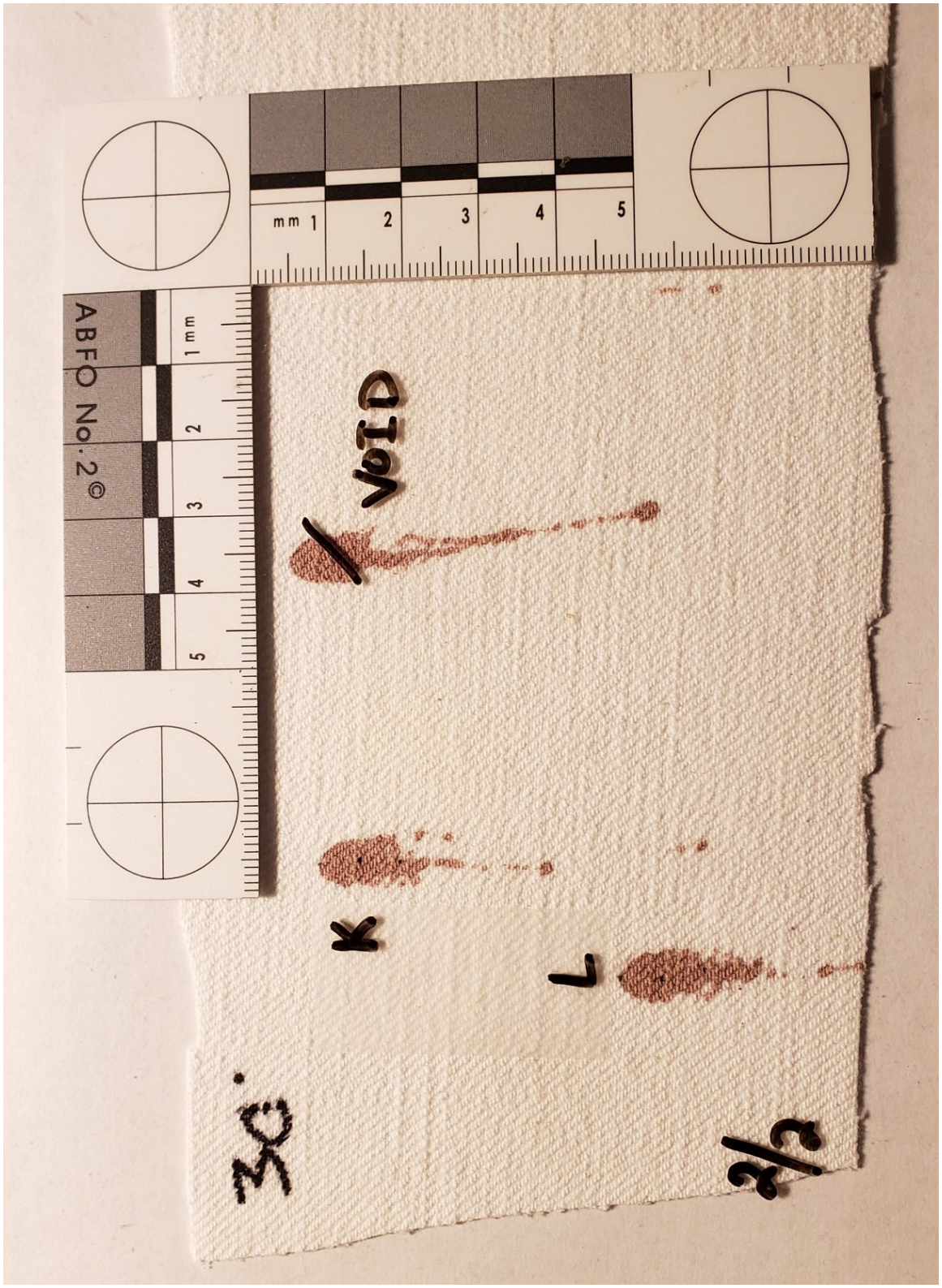
mm 1 2 3 4 5
ABFO No. 2©
1 mm 2 3 4 5
VOID
K
L
30°
2/2

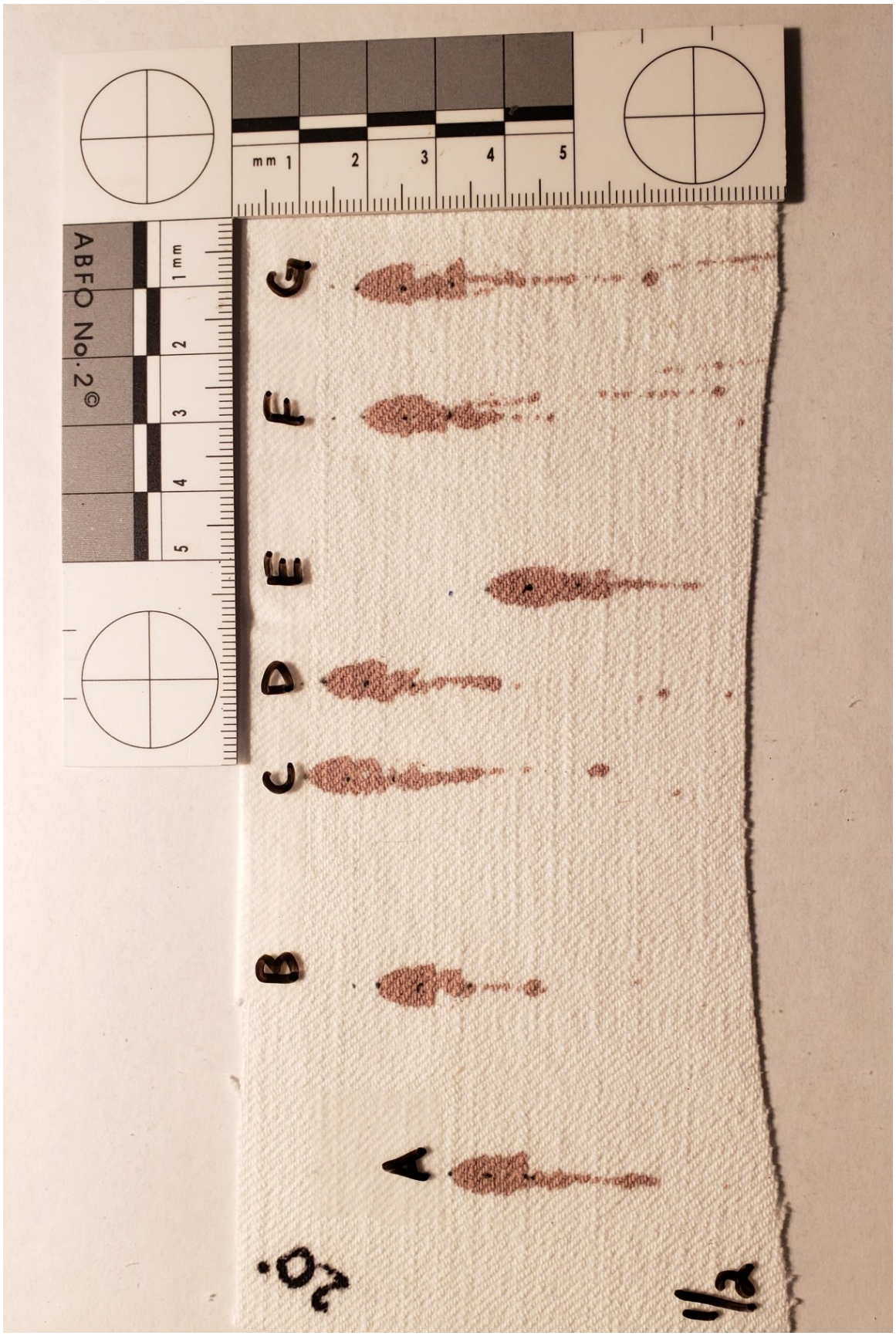
mm 1 2 3 4 5
ABFO No. 2©
1 mm 2 3 4 5
G
F
E
D
C
B
A
20°
1/2

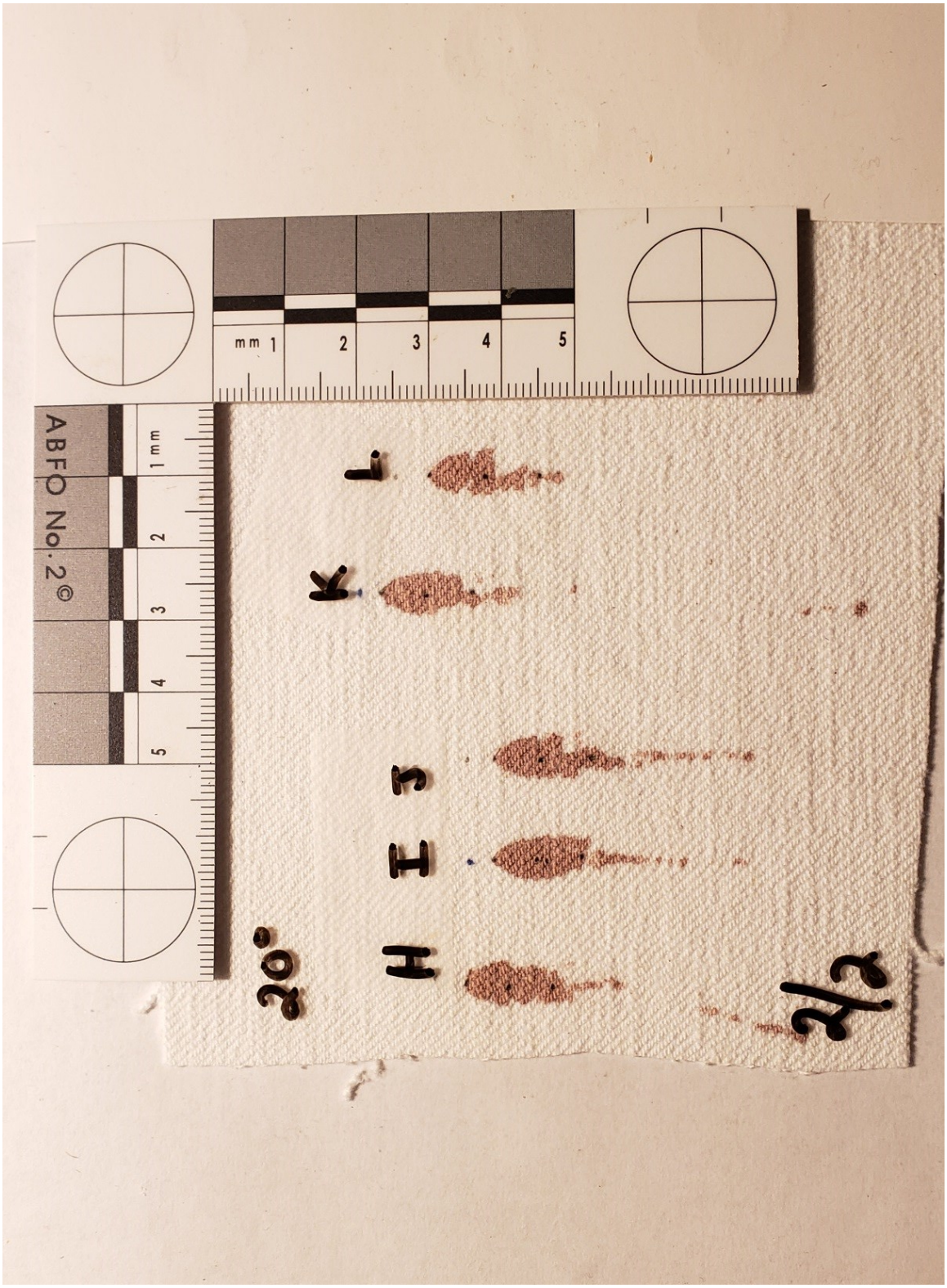
mm 1
2
3
4
5
ABFO No. 2©
1 mm
2
3
4
5
20°
45°

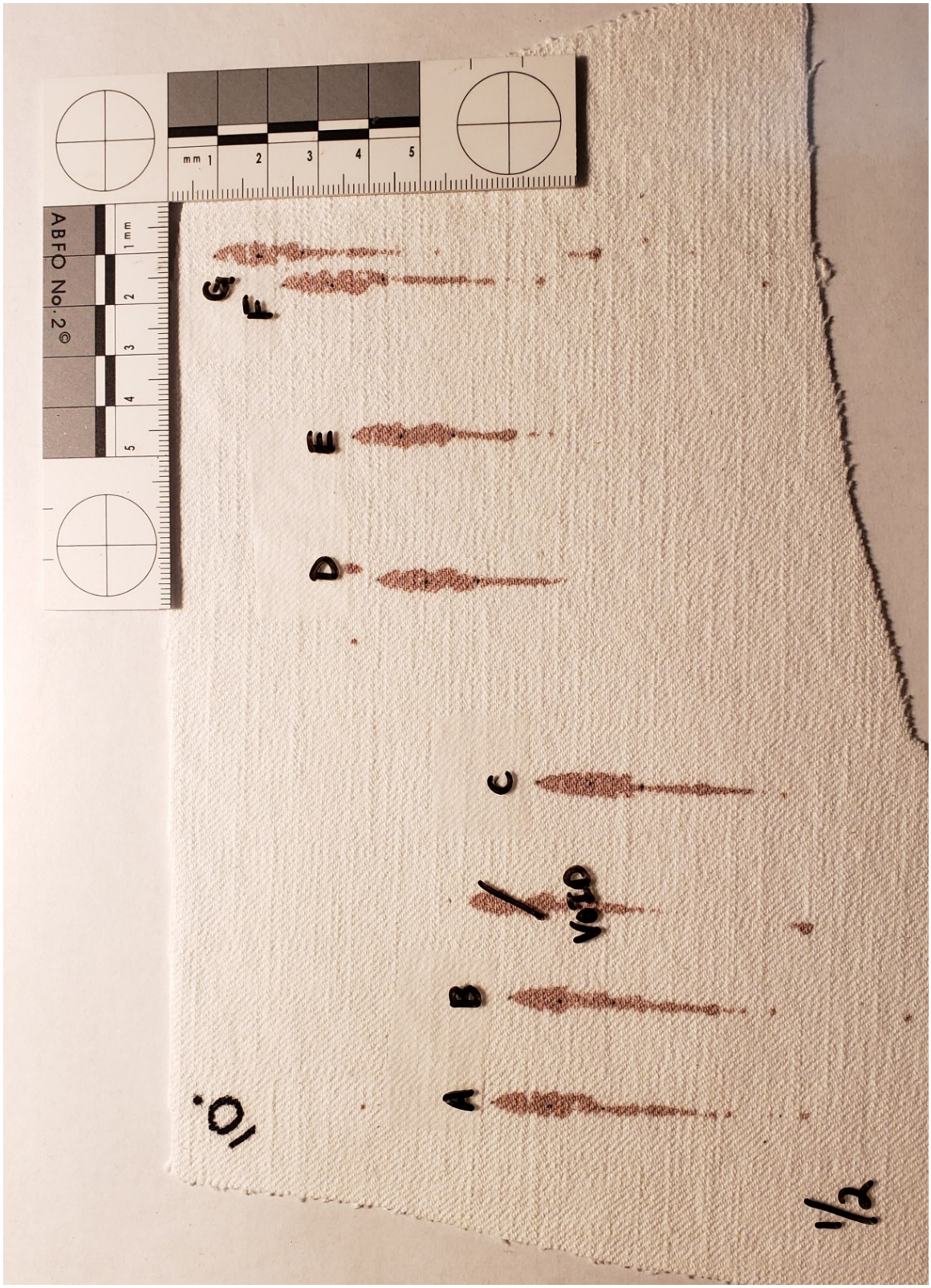
ABFO No. 2©
mm 1 2 3 4 5
1 mm 2 3 4 5
G
F
E
D
C
B
A
10.
1/2

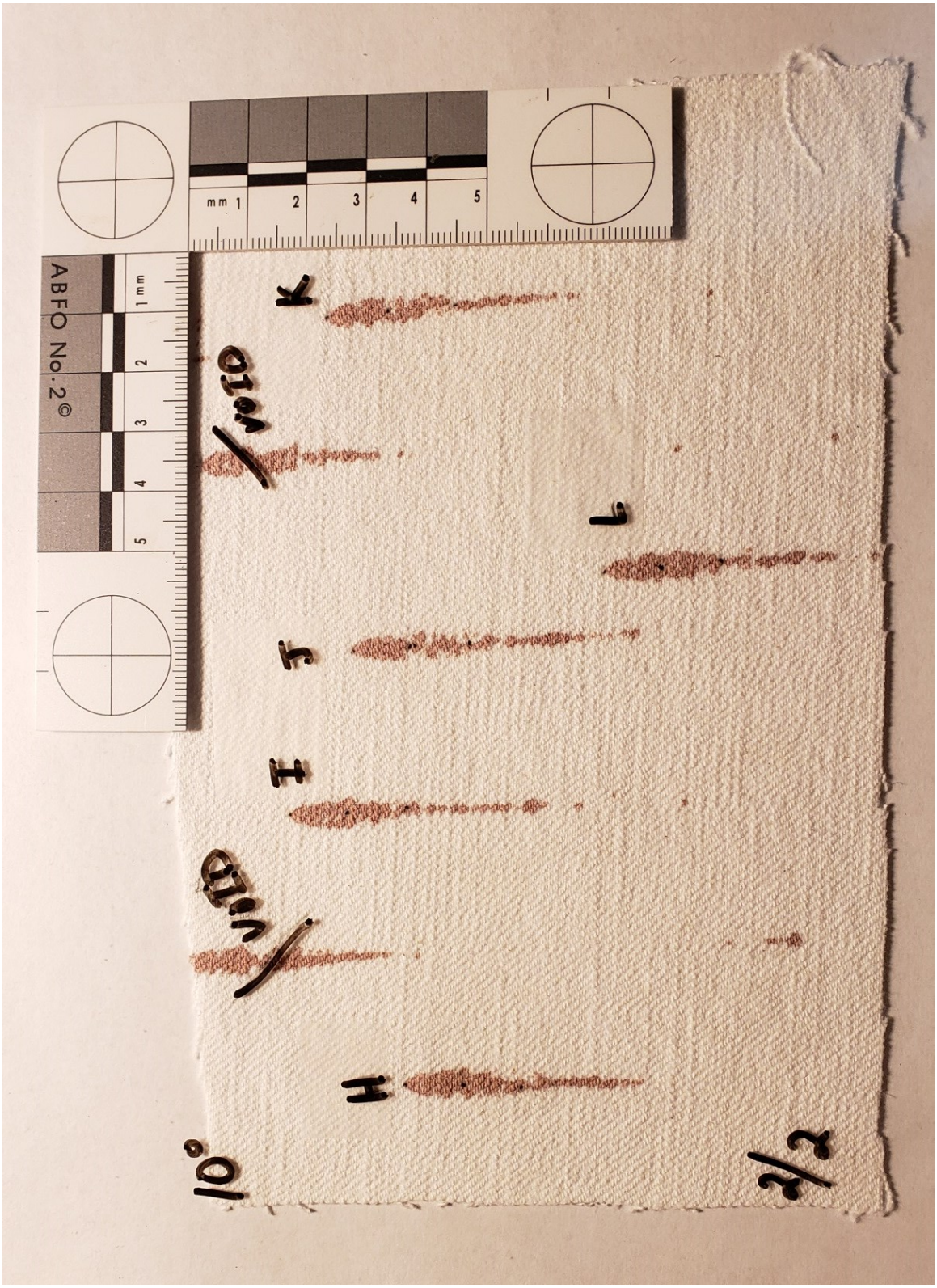
ABFO No. 2©
mm 1
2
3
4
5
1mm
2
3
4
5
K
J
I
H
10°
22°